ACS Catalysis

pubs.acs.org/acscatalysis

Research Article

On the Mechanism and Selectivity of Palladium-Catalyzed C(sp^3)−H Arylation of Pyrrolidines and Piperidines at Unactivated C4 Positions: Discovery of an Improved Dimethylaminoquinoline Amide Directing Group

Daniele Antermite, Andrew J. P. White, Luis Casarrubios, and James A. Bull*

Cite This: *ACS Catal.* 2023, 13, 9597−9615

Read Online

ACCESS | Metrics & More | Article Recommendations | Supporting Information

ABSTRACT: Directed C−H functionalization is a powerful means to functionalize otherwise unreactive C−H bonds, for which aminoquinoline amides provide a powerful and frequently used directing group. Saturated N-heterocycles are crucial motifs in medicinal chemistry. However, the C−H functionalization of N-heterocycles has posed considerable challenges, often giving incomplete conversions. On unsymmetrical substrates, poorly understood regio- and stereoselectivity considerations have prevented more forcing conditions and further limited yields. Here, we present a combined experimental and computational study on the regio- and stereoselective C4 arylation of pyrrolidines and piperidines with C3 aminoquinoline amide directing groups. Detailed mechanistic experiments are presented including deuteration, kinetics investigations, and isolation of palladacycles. Palladacycle formation is reversible and proceeds preferentially at C4, though activation of both C−H bonds at C4, *cis* and *trans* to the directing group, occurs equally. The *cis*-selectivity results from strain in the *trans*-palladacycle ($\Delta\Delta G_{trans-cis}$ ~6 kcal mol^{-1}), which is retained in subsequent transition states. Hence, the oxidative addition step is stereo-determining. However, the turnover-limiting step for the catalytic cycle is reductive elimination, and reduced rates and yields are observed with electron-poor aryl iodides. Importantly, kinetics experiments reveal a rapid loss of the active Pd catalyst, likely due to the buildup of iodide, and a role for K_2CO_3/PivOH in catalyst turnover. Finally, we present the discovery of an improved 4-dimethylamine-8-aminoquinoline directing group (DMAQ). This removable auxiliary achieves >2× rate acceleration, generally improved yields, as well as improved *cis*-selectivity, by promoting reductive elimination. A broad reaction scope of aryl iodides is demonstrated, including the late-stage functionalization of drug compounds which is enabled by the use of only one equivalent of functionalized iodides.

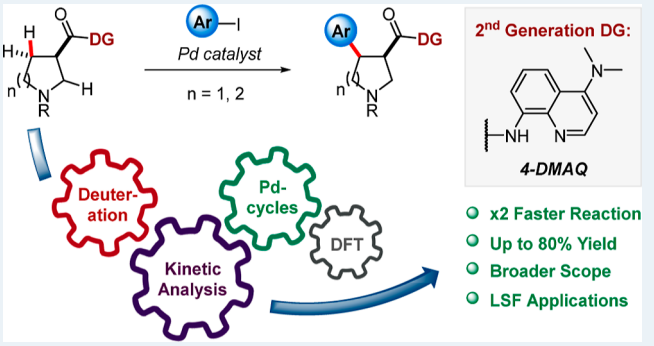

KEYWORDS: *palladium, C−H functionalization, heterocycles, mechanism, selectivity, kinetics, late-stage functionalization*

INTRODUCTION

Developments in C−H functionalization continue to provide exciting new disconnections for the synthesis of valuable compounds in drug discovery and materials science.[1] These methods present opportunities both for increased synthetic efficiency and for the divergent and iterative preparation of compounds in discovery chemistry. This is notable in the pharmaceutical industry where many iterations are required to optimize compound properties. Saturated N-heterocycles present extremely common substructures in medicinal compounds, most notably piperidine and pyrrolidine rings (Figure 1a).[2] Regio- and stereocontrolled synthesis of such heterocycles is therefore important in the development of new drugs and continues to receive enormous synthetic attention.[3] The conceptual simplicity of attaching substrates directly to the intact rings by C−H functionalization is an attractive goal, especially to exploit the numerous potential of 3D exit vectors from the saturated ring structures.[4,5]

The advent of amide directing groups provided a major advance in the development of C−H functionalization methods.[6−9] Seminal reports from Yu[8] and Daugulis[9] of mono- and bidentate amide directing groups, respectively, removed the reliance of intrinsic directing groups on a substrate and allowed their subsequent modification to a much broader range of polar functionality (Figure 1b).[10]

Received: May 3, 2023
Revised: June 12, 2023
Published: July 7, 2023

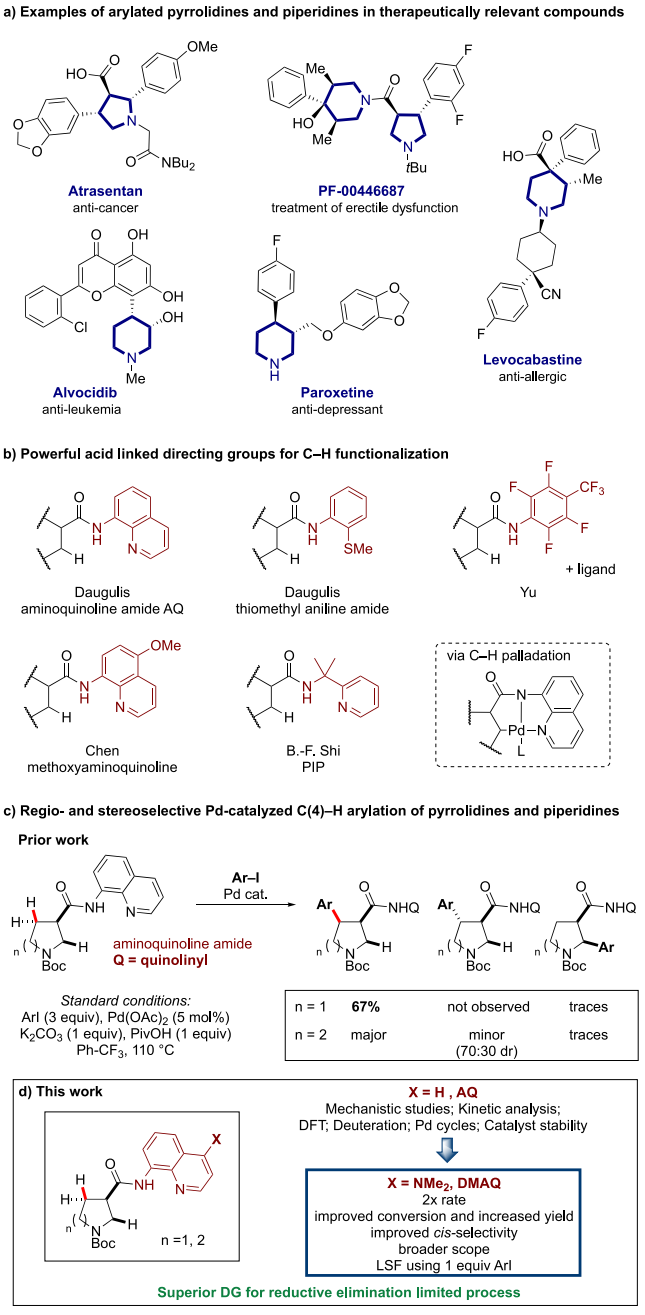

Figure 1. (a) N-Heterocycles in medicinal compounds. (b) Acid-linked amide directing groups for C−H functionalization. (c) Previous work on the regio- and stereoselective C−H arylation of pyrrolidines and piperidines. (d) This work: detailed mechanistic studies on heterocycle C−H arylation with the aminoquinoline directing groups and the development of an improved DMAQ directing group.

Perhaps the most widely used one has been the bidentate 8-aminoquinoline (AQ) amide directing group introduced by Daugulis for sp^2 and sp^3 arylation where the bidentate directing group prevents β-hydride elimination.[9a,b] Aminoquinoline amides have been subsequently exploited extensively for a wide range of applications and continue to see new transformations employing a range of transition-metal catalysts.[11−13] Various alternative carboxylic acid-linked directing groups have emerged, for example, thiomethylaniline,[14] and Shi's PIP (2-(pyridine-2-yl)isopropyl) amide group[15] which have both seen significant applications.[16] It is noticeable that the aminoquinoline amide itself has seen little variation since its introduction in 2005, with the unsubstituted aminoquinoline used primarily. Notably, Chen developed 5-methoxy-8-aminoquinoline to facilitate oxidative removal[17] and studied the performance of different derivatives in mediating enantioselective reactions.[18,19] Broader implications of electronic changes to the aminoquinoline are not well studied.

More generally in palladium-catalyzed C−H functionalization, there is limited understanding of the mechanistic basis that dictates regio- and stereoselectivity when multiple C−H sites are available at the same distance from the directing group. Reactions with bidentate directing groups typically operate through a Pd^{II}/Pd^{IV} mechanism,[20,21] commonly involving concerted metalation deprotonation with a Pd^{II} species benefiting from carboxylate and related additives.[22] There remains little known about the turnover-limiting steps in the majority of these processes. Observations on the relative success of aryl iodides with different electronic features give a mixed picture, and there are examples of C−H activation or oxidative addition/reductive elimination steps being turnover-limiting, though often not well distinguished.[23−25] This limited mechanistic detail hampers the development of improved processes, especially those involving subtle selectivity features.

The first report of palladium-catalyzed C−H arylation of N-heterocycles was from our lab in 2014 on proline aminoquinoline amide, which achieved *cis*-C3 arylation.[26] Piperidine,[27] azetidine,[28] and other ring sizes with C2 directing groups have since been successfully arylated.[4,29,30] Maes reported the arylation of amine-linked piperidine C3 picolinamide,[31] we reported the use of a C4 aminoquinoline amide directing group on piperidines,[32] and Sanford reported the C4 arylation of piperidine derivatives with an *N*-linked directing group.[33,34]

In 2018, we developed the C4 functionalization of pyrrolidines and piperidines with a C3 aminoquinoline amide directing group (Figure 1c).[35] This work displayed selectivity for C4 on both the 5- and 6-ring derivatives and gave *cis*-selectivity in both cases, with a minor *trans*-product also formed only for the piperidines (Figure 1c). Although useful yields were obtained for the *cis*-substituted products, a plateau at 60−70% conversion was observed. More forcing conditions did not improve conversions and gave reduced selectivity. Furthermore, these processes gave low yields with electron-poor aryl iodides. Nonetheless, this methodology was applied to the preparation of enantiopure (−)-paroxetine derivatives to study the paroxetine serotonin transporter (SERT) binding site.[36]

Given the value of the N-heterocycle products and the difficulty in achieving full conversion due to the required selectivity and other limitations on the process, we identified that this transformation represented a very interesting opportunity to gain more insights into the regio- and stereoselectivity requirements for directed C−H functionalization reactions that could be of general use. Additionally, we aimed to use the mechanistic insight to overcome previous limitations, specifically (i) the low yields with aryl iodides bearing electron-withdrawing groups resulting in a limited scope and (ii) the general plateau in conversion.

Here, we describe detailed experimental and computational investigations into the mechanistic features and the origin of both the regio- and stereochemical outcomes for 5- and 6-

https://doi.org/10.1021/acscatal.3c01980
ACS Catal. 2023, 13, 9597−9615

membered heterocycles with C3 directing groups (Figure 1d). Mechanistic and kinetic investigations provide insights into each step of the process and how these influence the reaction outcomes. Previous limitations are overcome with the development of a new 4-dimethylamine-8-aminoquinoline (DMAQ) amide directing group, which achieved improved yields and broader reaction scope.

RESULTS AND DISCUSSION

C−H Activation Step. We began the study by using deuterium labeling experiments to probe the C−H activation step independently from the overall catalytic cycle. Treating *N*-Cbz piperidine **1** with catalytic $Pd(OAc)_2$ and excess AcOD-d_4 led to deuterium incorporation at three positions β- to the directing group (Scheme 1a).[37] Increased deuteration was observed at C4 compared to the C2-position, despite the stronger C(4)−H bond, in line with the regioselectivity of C−H arylation.[35] At C2, deuteration was observed exclusively at the *cis*-position. However, both *cis*- and *trans*-C(4)−H bonds were deuterated extensively (75% D and 66% D, respectively). Subjecting the 5-membered ring pyrrolidine-3-carboxamide **2** to the same conditions gave similar regio- and stereochemical outcomes (Scheme 1b). Reaction at C4 was again favored over C2, resulting in 88% D incorporation at both *cis*- and *trans*-C(4)−H positions. Monitoring the D-labeling over time by ^{1}H NMR indicated that deuteration of *cis*- and *trans*-C(4)−H positions proceeded at a similar rate, while C(2)−H deuteration was much slower and resulted in lower levels of D incorporation (Scheme 1c). The observation of pyrrolidine *trans*-deuteration was surprising as it corresponds to the *trans*-fused 5,5-palladacycle and *trans*-arylation does not occur. Prior studies on proline substrates indicated only *cis*-deuteration, though cyclopentyl amides have shown *cis*- and *trans*-deuteration.[38] The final isotopic distribution was independent of the *N*-protecting group, with similar results obtained with a smaller methyl carbamate substituent, indicative that the Boc group is not required for steric reasons.[39] No deuteration was found at C3 for either the piperidine or pyrrolidine ring, ruling out potential acid-mediated enolization. In addition, no reaction occurred in the absence of a Pd catalyst. Together, this was suggestive of a reversible cleavage of both *cis*- and *trans*-C(4)−H bonds, forming *cis*- and *trans*-cyclopalladated intermediates regardless of the ring size. The formation of *trans*-6-membered palladacycles has previously been proposed for cyclohexane and tetrahydropyran systems bearing an 8-AQ amide directing group[38,40] and is consistent with the diastereomeric mixture of piperidine products formed in the reaction with aryl iodides.

Scheme 1. (a) Pd-Catalyzed C−H Deuteration of Piperidine 1; (b) Pd-Catalyzed C−H Deuteration of Pyrrolidine 2;[a] (c) Deuterium Incorporation (%) at Different Positions of Pyrrolidine 2 as a Function of Time[b]

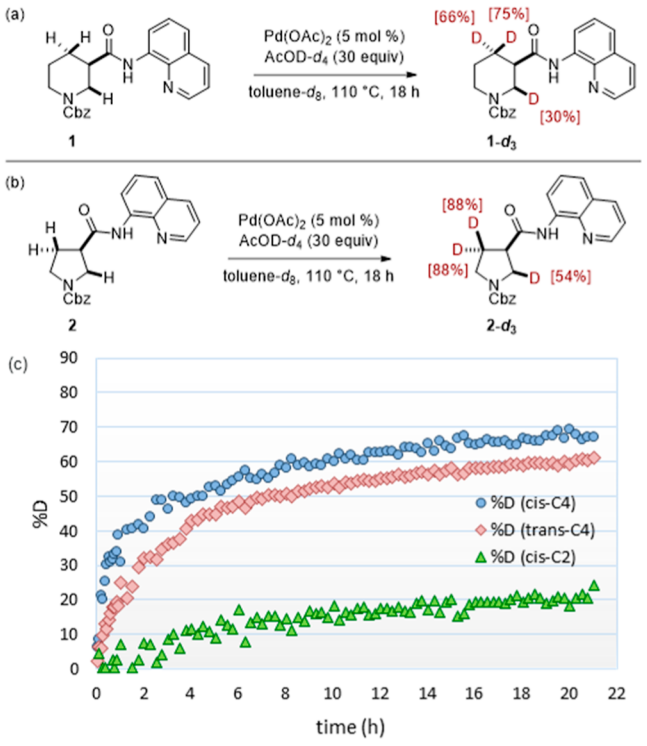

[a]% D determined by quantitative ^{1}H NMR in DMSO-d_6 at 100 °C. [b]Determined by quantitative ^{1}H NMR in toluene-d_8 at 100 °C.

In recent years, hydrogen−deuterium exchange has attracted significant attention in pharmaceutical research, enabling powerful diagnostic and analytical tools, as well as providing access to drug candidates with advantageous pharmacokinetic properties.[41] As such, this catalytic C−H deuteration itself offers potential for the synthesis of D-labeled pyrrolidine and piperidine fragments and building blocks for drug discovery. Deuterated pyrrolidine **2**-d_3 was isolated in an 83% yield and ≥90 %D at *cis*-C(2), *cis*-C(4), and *trans*-C(4), upon two consecutive deuteration cycles.[39,42]

With this fully labeled derivative in hand, we examined any kinetic isotope effect (KIE) of C(4)−H arylation. Consistent with a reversible C−H activation step, partial H/D scrambling was observed when subjecting **2**-d_3 to the standard arylation conditions in the absence of aryl iodide.[39] On the other hand, no detectable D incorporation was found upon treatment of pyrrolidine **2** with $Pd(OAc)_2$ and K_2CO_3/AcOD-d_4 in toluene-d_8. Reasoning that this could be due to the acidic amide acting as a proton source, pyrrolidine **2**-d_4 was synthesized via H/D exchange in MeOD-d_4 (Scheme 2).[39] Pleasingly, when subjecting **2**-d_4 to the arylation conditions, no erosion in % D was observed in the substrate. As such, this derivative was used for KIE evaluation. The initial rate of C−H arylation for proteo- and deutero-pyrrolidines **2** and **2**-d_4 was first compared in independent experiments (Scheme 2a). Similar individual rate constants were observed (k_H = 1.19 ± 0.13 mM min^{-1} and k_D = 0.99 ± 0.15 mM min^{-1}), resulting in a small KIE of 1.20. Similarly, no large primary isotope effect was found when **2** and **2**-d_4 competed for a limiting amount of 4-iodoanisole (Scheme 2b). These results indicated that the C−H activation step is not turnover-limiting. At the same time, the small positive KIE value could be ascribed to an equilibrium isotope effect, consistent with a reversible C−H bond cleavage.[43]

Stoichiometric experiments were then performed to isolate the relevant palladacycle intermediates after C−H activation. Attempts to react pyrrolidine **2** with $Pd(OAc)_2$ in Ph-CF_3, *t*-amyl-OH, or MeCN failed to deliver any isolable Pd(II)-complex. Reasoning that this process could be thermodynamically unfavorable, the use of stabilizing ligands was evaluated. Pleasingly, using 2.2 equiv of pyridine afforded monomeric complex **4-Py** in a 66% yield as a single diastereomer with Pd exclusively at C4 (Scheme 3). A relative *cis*-configuration of the pyrrolidine ring was first assigned based on 2D NOESY NMR

https://doi.org/10.1021/acscatal.3c01980
ACS Catal. 2023, 13, 9597−9615

Scheme 2. KIE for Pyrrolidine C(4)−H Arylation in (a) Parallel Rate Experiments and (b) Intermolecular Competition Experiments[a]

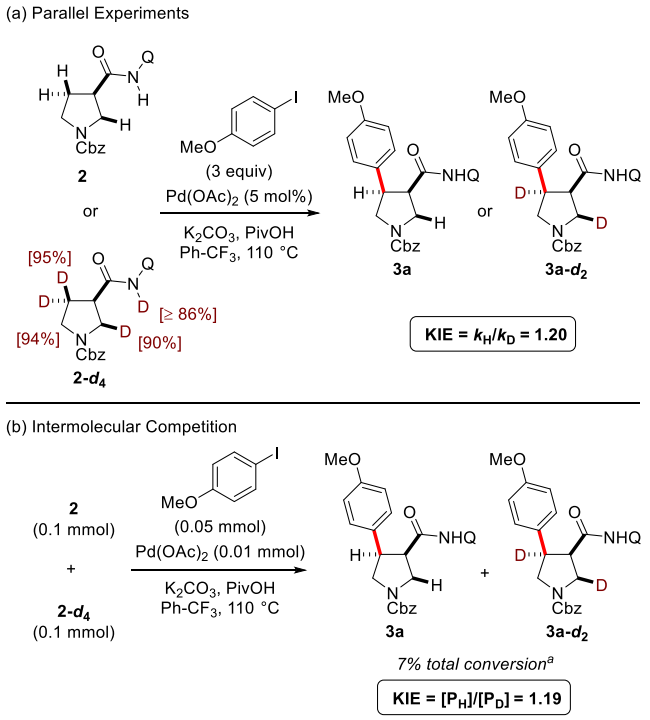

[a]Determined by ^{1}H NMR using 1,3,5-trimethoxybenzene as the internal standard. Q = quinolin-8-yl.

Scheme 3. Synthesis of Mononuclear 5,5-*cis*-Palladacycle Complexes 4-Py and 5-PCy$_3$[a]

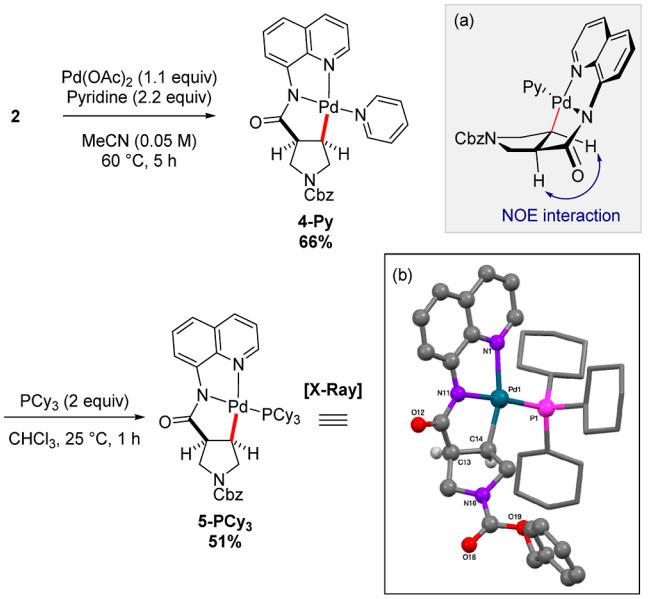

[a](a) *cis*-Configuration of **4-Py** determined by NOESY NMR. (b) Crystal structure of palladacycle **5-PCy$_3$**. Hydrogens are omitted for clarity, except for those at the ring junction (C13 and C14).

and then unambiguously confirmed by X-ray diffraction after ligand exchange with tricyclohexylphosphine (Scheme 3b).

The X-ray structure of **5-PCy$_3$** showed the pyrrolidine ring to adopt an envelope conformation, where the Pd center and the amide substituents occupy pseudoequatorial and pseudoaxial positions, respectively. A slightly distorted square planar geometry was found at Pd, confirming the bidentate coordination of the AQ auxiliary.

The reactivity of complex **4-Py** was investigated under both deuteration and arylation conditions.[39] Unfortunately, the use of 35 wt % DCl resulted in complete degradation at room temperature, while just unreacted **4-Py** remained after 18 h at reflux in MeOD-d_4. On the other hand, deuteration of both *cis*- and *trans*-C(4) positions was observed using AcOD-d_4 in toluene-d_8 at 110 °C, likely due to Pd(OAc)$_2$ being generated in situ. Importantly, complex **4-Py** was a competent catalyst in the C−H arylation of pyrrolidine **2**, giving the desired product in a 49% yield under otherwise standard conditions. Finally, stoichiometric arylation of **4-Py** with 4-iodoanisole gave the corresponding 4-arylated product as a single *cis*-diastereomer. In this case, a lower 13% yield was obtained, likely due to both a detrimental effect of stoichiometric pyridine and the more stabilized palladacycle. Together, this suggested that closely related palladacycles bearing a carboxylic acid ligand instead of pyridine are likely active intermediates in the reaction of pyrrolidine 3-carboxamides.

Kinetic Investigations into Oxidative Addition and Reductive Elimination. Having established that the C−H bond cleavage is neither stereo-determining nor turnover-limiting, we turned our attention to the subsequent oxidative addition and reductive elimination steps. Initially, we used Burés' variable time normalization analysis (VTNA) to determine the kinetic order in each reaction component.[44] The formation of arylated product **7a** was monitored over time using different initial loadings of Pd(OAc)$_2$, aryl iodide, or pyrrolidine substrate (Figure 2). Evaluation of the reaction profile under standard conditions (green diamonds) revealed a fast initial conversion, giving **7a** in a 19% yield after just 30 min[39] However, the rate of arylation decreased progressively, reaching a plateau at 5−6 h. Unreacted pyrrolidine **6** accounted for the remaining mass balance almost entirely, suggesting product inhibition or other catalyst deactivation processes (vide infra). Assuming such effects to be less pronounced in the first stages of the reaction, earlier time points (up to 45 min) were considered to evaluate the order in Pd(OAc)$_2$ (Figure 2a). Faster formation of product **7a** was observed at higher catalyst loadings, resulting in four nonoverlapping concentration traces. Normalization of the timescale for Δt [cat]^n gave an optimal fitting of all profiles with n = 1 (Figure 2d).[44a]

This indicated a first-order dependence in the catalyst, consistent with a mononuclear Pd species being involved in the turnover-limiting step. A positive correlation was also found between equivalents of 4-iodoanisole and reaction rate (Figure 2b). Timescale normalization revealed a clear profile overlap with the power α equal to 1, reflecting a first order in aryl iodide (Figure 2e).[44b] On the other hand, decreasing the initial concentration of substrate **6** did not affect the rate of product formation, and overlap was observed only for α = 0 (Figure 2c,f). The reaction rate was also independent of the loading of K_2CO_3 and PivOH, though this influenced the final conversion.[39] Finally, no significant difference in the reaction outcome was found with different stirring rates, ruling out a potential mass-transfer effect.[39] Overall, this was consistent with either oxidative addition or reductive elimination as the turnover-limiting step, while the observed zero-order dependence in **6** could likely be ascribed to catalyst saturation under

https://doi.org/10.1021/acscatal.3c01980
ACS Catal. 2023, 13, 9597−9615

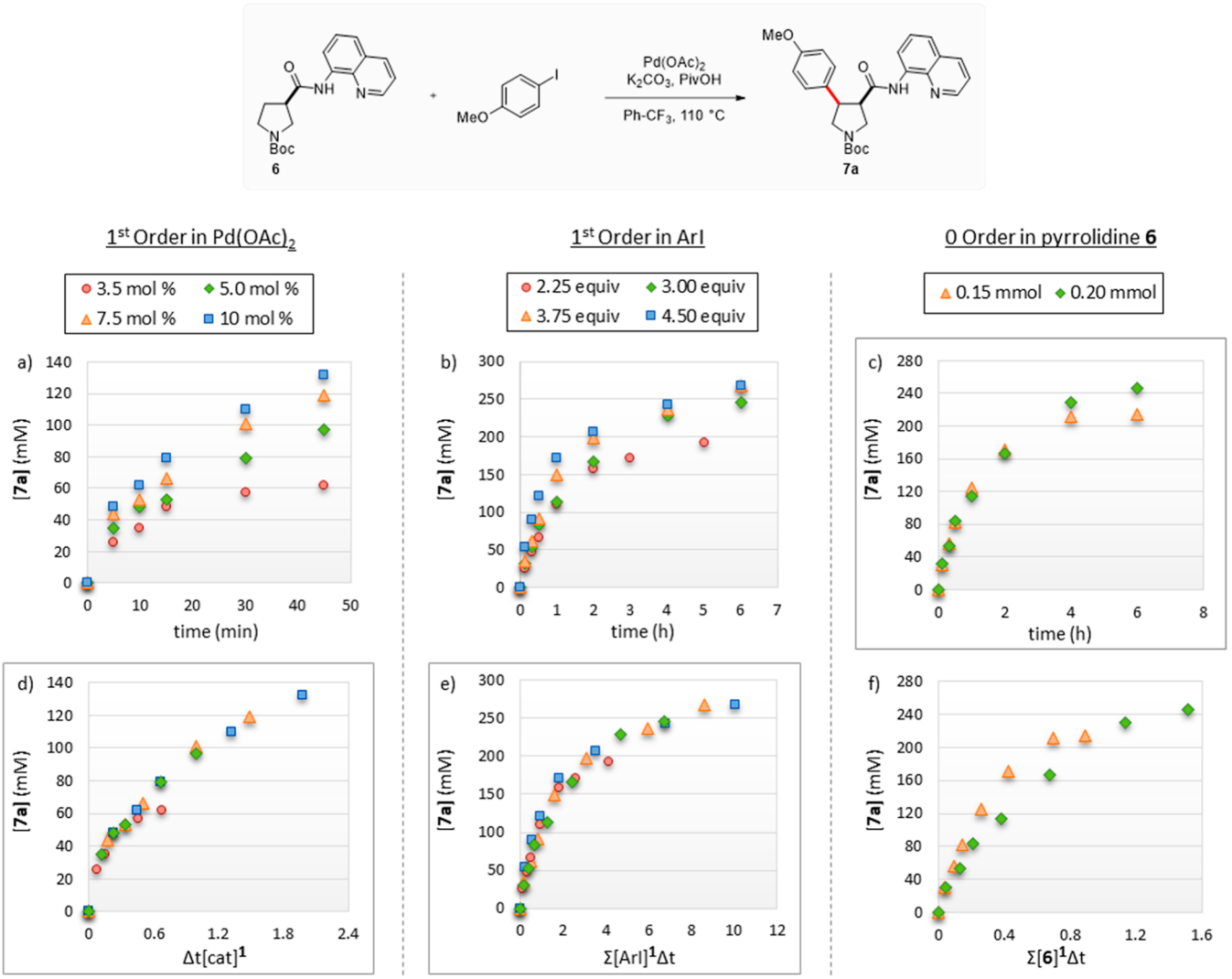

Figure 2. Use of VTNA to determine the reaction order in $Pd(OAc)_2$, ArI, and pyrrolidine **6**. The profiles obtained under standard conditions are represented by green diamonds. Top row: concentration of product **7a** as a function of time using different initial concentrations of (a) $Pd(OAc)_2$, (b) Ar−I, and (c) substrate **6**. Each data point corresponds to a discrete reaction. Bottom row: concentration profiles of **7a** after timescale normalization for the first order in (d) $Pd(OAc)_2$, (e) Ar−I, and (f) **6**. Reaction conditions: (a) **6** (0.2 mmol), ArI (0.6 mmol), $Pd(OAc)_2$ (7−20 μmol), K_2CO_3 (0.2 mmol), PivOH (0.2 mmol), $PhCF_3$ (200 μL); (b) **6** (0.2 mmol), ArI (0.45−0.9 mmol), $Pd(OAc)_2$ (10 μmol), K_2CO_3 (0.2 mmol), PivOH (0.2 mmol), $PhCF_3$ (200 μL); (c) **6** (0.15−0.2 mmol), ArI (0.6 mmol), $Pd(OAc)_2$ (10 μmol), K_2CO_3 (0.2 mmol), PivOH (0.2 mmol), $PhCF_3$ (200 μL).

the synthetically relevant conditions, i.e., a catalyst resting state involving a Pd−substrate complex.[45]

Expecting opposite electronic requirements for the aryl iodide reactant in the oxidative addition and reductive elimination steps, the effect of different *para*-substituted iodoarenes was investigated. In typical Pd(0)/Pd(II)-catalyzed reactions, the oxidative addition step is well known to benefit from electron-rich ligands to increase electron density on Pd and electron-poor aryl iodides to help withdraw electron density.[46,47] The reductive elimination step reverses these electronic requirements. In Pd(II)/Pd(IV) processes, the demands of these steps on the aryl iodide electronics are less clearly defined.[21,48,49] Competition experiments between two different aryl iodides for a limiting amount of pyrrolidine **6** revealed a faster reaction with more electron-rich coupling partners (Scheme 4a). Individual kinetic profiles also showed a faster rate with more electron-rich aryl iodides and gave a linear Hammett dependence with a negative slope (Scheme 4b).[39] A better correlation was obtained using electrophilic substitution constants σ_p+, rather than σ_p values, suggesting the involvement of mesomeric effects.[50] The negative Hammett correlation was consistent with the formation of a partial positive charge in the turnover-limiting transition state, which could be stabilized by electron-donating substituents in direct conjugation. Consequently, we interpreted this to support reductive elimination, rather than oxidative addition, as the turnover-limiting step of the reaction.

Computational Analysis. To corroborate the experimental data, the mechanism of C−H arylation of pyrrolidine-3-AQ amide was examined by density functional theory (DFT) calculations (Figure 3). A slightly simplified system was chosen to model the experimental conditions, involving $Pd(OAc)_2$, toluene as the solvent, and methyl carbamate as an *N*-protecting group.[51] Initial catalyst coordination to the AQ auxiliary resulted in the exergonic formation of acetic acid and Pd-complex **I-1**, which was taken as the starting point to

https://doi.org/10.1021/acscatal.3c01980
ACS Catal. 2023, 13, 9597−9615

Scheme 4. (a) Competition Experiments with *para*-Substituted Aryl Iodides;[a] (b) Hammett Plot of log (k_X/k_H) as a Function of σ_p+

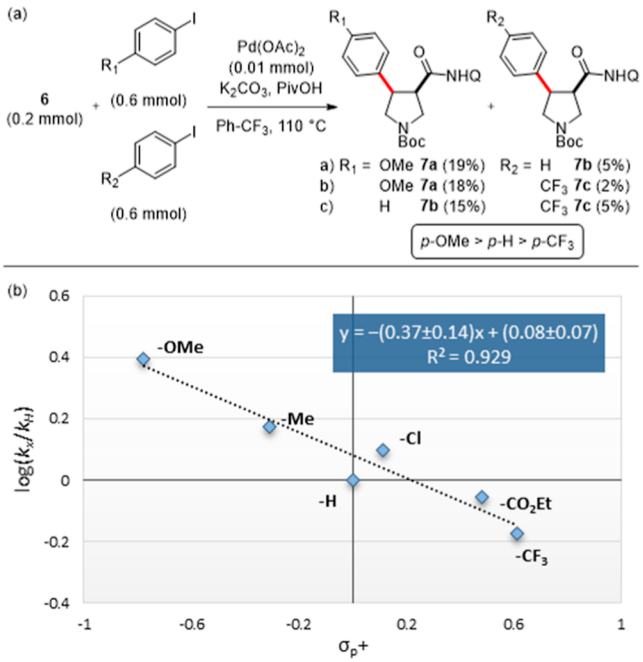

[a]Determined by ^{1}H NMR using 1,3,5-trimethoxybenzene as the internal standard. Q = quinolin-8-yl.

investigate the subsequent steps, as in previous studies.[23b,24,33,52] Amide complex **I-1** was considered to be the resting state of the catalytic cycle, consistent with the zero-order kinetics observed in the pyrrolidine substrate.[33b,45,53] A direct oxidative addition of iodobenzene to **I-1** was found to be energetically unviable, similar to reported computational studies involving aryl bromides.[24,39] In contrast, an inner-sphere concerted metalation deprotonation (CMD) event was found to be feasible at both *cis*- and *trans*-C(4)−H positions, whereby the acetate ligand acted as an internal base for C−H cleavage with simultaneous formation of the C−Pd bond (Figure 3a).[22]

Very similar energetic barriers were observed for the corresponding transition states **TS-CH**$_{cis}$ and **TS-CH**$_{trans}$ ($\Delta G^{‡}$ = 24.9 and 24.2 kcal mol^{-1}, respectively), consistent with the stereochemical outcome of C−H deuteration. Cleavage of the *trans*-C(4)−H bond was allowed only with a pseudoequatorial orientation of the AQ auxiliary, while the lowest energy pathway for *cis*-C(4)−H activation involved a pseudo-axial arrangement of the directing group (Figure 3b). C−H activation afforded *cis*- and *trans*-palladacycle intermediates **I-2**$_{cis}$ and **I-2**$_{trans}$, exhibiting a slightly distorted square planar geometry at the Pd center (Figure 3a). **I-2**$_{cis}$ and **I-2**$_{trans}$ were found to be 8.3 and 14.5 kcal mol^{-1} uphill from **I-1**, respectively. This was in line with the experimental evidence for a quasi-reversible C−H activation step, which failed to afford any isolable palladacycle without exogenous ligands. In addition, the isolation of palladacycle **4-Py** as a single *cis*-diastereomer (cf. Scheme 3) was consistent with the thermodynamic stability of **I-2**$_{cis}$ ($\Delta\Delta G_{trans-cis}$ = 6.2 kcal mol^{-1}).[54] This is likely due to the higher strain of the *trans*-5,5-bicyclic system in **I-2**$_{trans}$. An alternative outer-sphere CMD mechanism was also contemplated,[23b,55] but calculations pointed instead to a new inner-sphere process with associated energies that could not compete with that proposed in Figure 3a and was thus discarded.[39] The feasibility of an inner-sphere CMD event at *cis*-C(2) was also evaluated, but no conclusive energetic discrimination could be ascertained versus *cis*-C(4) ($\Delta\Delta G_{C2-C4}$ < 1 kcal mol^{-1}).[39] From **I-2**$_{cis}$ and **I-2**$_{trans}$, oxidative addition was then evaluated using iodobenzene as a model substrate. Acetic acid dissociation followed by iodide coordination allowed oxidative addition to occur through 3-membered transition states **TS-OA**$_{cis}$ and **TS-OA**$_{trans}$ (Figure 3a). This gave penta-coordinated complexes **I-3**$_{cis}$ and **I-3**$_{trans}$. Once the C−H bond is activated to obtain the *cis*- and *trans*-palladacycles **I-2**$_{cis}$ and **I-2**$_{trans}$, the reaction has a clear energetic preference for the *cis*-based pathway which is maintained until the final products. Oxidative addition is therefore the stereo-determining step with **TS-OA**$_{trans}$ calculated to be 6.9 kcal mol^{-1} higher in energy than **TS-OA**$_{cis}$.[54,56,57] This energy difference is baked in from the palladacycle formation, resulting in exclusive formation of *cis*-arylated products. Reductive elimination from the Pd(IV) complexes occurred through unsaturated square-pyramidal transition states **TS-RE**$_{cis}$ and **TS-RE**$_{trans}$, forming the new C−C bond. Halide abstraction and protodemetalation would finally give the arylated product and allow catalyst turnover. In the *cis*-arylation pathway, a similar energetic barrier was found for oxidative addition and reductive elimination steps ($\Delta G^{‡}$ = 32.3 and 33.9 kcal mol^{-1}, respectively). In this case, **TS-RE**$_{cis}$ resulted in 1.6 kcal mol^{-1} higher energy than **TS-OA**$_{cis}$, supporting the kinetic evidence for a turnover-limiting reductive elimination. On the other hand, the highest activation energy in the *trans*-pathway was associated with **TS-OA**$_{trans}$ ($\Delta G^{‡}$ = 39.2 kcal mol^{-1}).

To compare the reaction mechanism and selectivity features between different ring sizes, we also examined the C−H arylation of piperidine 3-carboxamide.[39] Equally facile C−H activation was again observed for both *cis*- and *trans*-C(4) positions through inner-sphere CMD, with **TS$_{pip}$-CH**$_{cis}$ being slightly favored over **TS$_{pip}$-CH**$_{trans}$. In contrast to the 5-membered ring, however, a much smaller energetic difference was found between *cis*- and *trans*-palladacycle intermediates ($\Delta\Delta G_{trans-cis}$ = 0.4 kcal mol^{-1}) as a result of the considerably reduced strain energy in 5,6-fused ring systems.[54] Interestingly, the highest energetic barrier for piperidine C−H arylation was found to be dependent on the geometry of the system (Figure 4). Easier oxidative addition with iodobenzene was observed for the *cis*-geometry ($\Delta\Delta G_{trans-cis}^{‡}$ = 3.9 kcal mol^{-1}), while reductive elimination was more facile for the *trans*-diastereomer ($\Delta\Delta G_{trans-cis}^{‡}$ = −1.9 kcal mol^{-1}). Nonetheless, comparable activation energy was observed for both pathways ($\Delta G_{cis}^{‡}$ = 31.1 kcal mol^{-1}; $\Delta G_{trans}^{‡}$ = 33.9 kcal mol^{-1}). This was consistent with the observed formation of major *cis*- and minor *trans*-arylated piperidine products.

Studies on Catalyst Deactivation. The rate of arylation of pyrrolidine **6** with 4-iodoanisole decreased progressively over time with a plateau at 5−6 h, at approx 60% conversion to product **7a**. We applied Blackmond's reaction progress kinetic analysis (RPKA) protocols to investigate the reasons for this stall in reactivity.[58] A "same-excess" experiment was applied to mimic the reaction at a later time point chosen as t = 1 h (approx half of the total conversion). Lower initial loadings of **6** and aryl iodide were used to match their concentrations after 1 h while keeping the same excess between them. The amount of base was also corrected by addition of the expected amount

https://doi.org/10.1021/acscatal.3c01980
ACS Catal. 2023, 13, 9597−9615

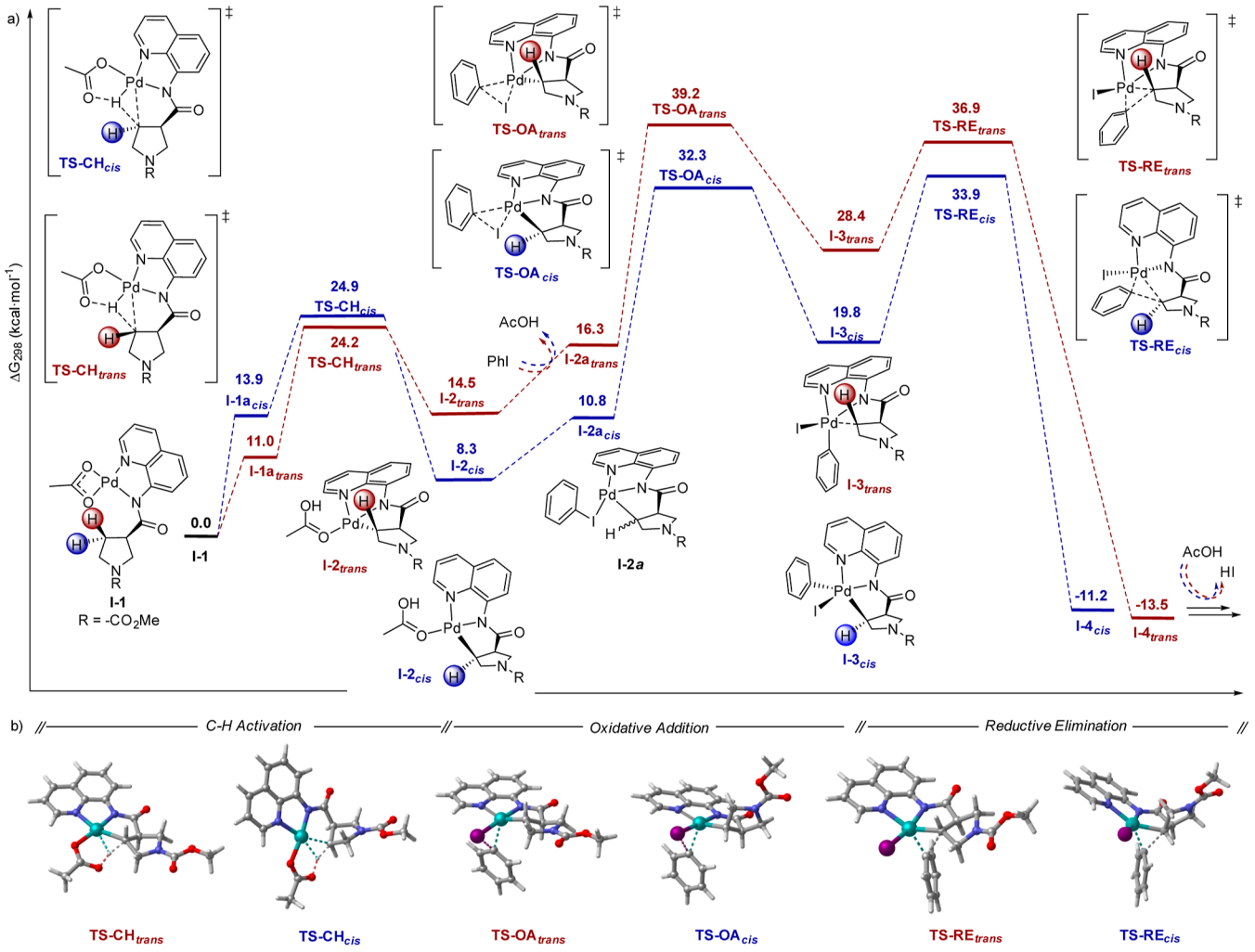

Figure 3. (a) Computational modeling of C−H arylation at *cis*- and *trans*-C(4) positions of pyrrolidine **I-1**. All free energy values (ΔG_{298} in kcal mol^{-1}) refer to the most stable conformation found for each intermediate and transition state, calculated at the CPCM(toluene)-DFT/m062x/Def2tzvpp level of theory. (b) Calculated structures for key transition states at the CPCM(toluene)-m062x/Def2tzvpp level. Images rendered with CYLview20.

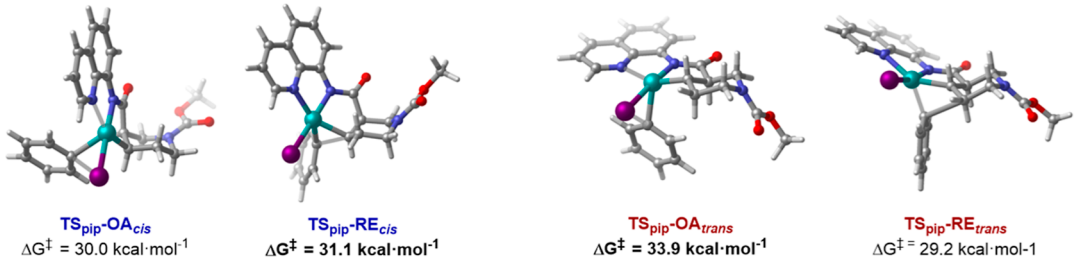

Figure 4. Calculated transition states for oxidative addition and reductive elimination on piperidine-3-AQ amide with iodobenzene. All free energy values (ΔG_{298} in kcal mol^{-1}) refer to the most stable conformation, calculated at the CPCM(toluene)-DFT/m062x/Def2tzvpp level of theory. Images rendered with CYLview20.

of $KHCO_3$ at t = 1 h. Timescale adjustment of the same-excess profile to the 1 h reference point revealed that the traces did not overlay, with a higher rate of substrate consumption compared to the standard reaction.[39]

To investigate the possibility of product inhibition as the reason for the nonoverlay, an additional same-excess plot was constructed with the addition of product **7a** at the concentration expected at 1 h.[39] Again, no visual overlap of the profiles was observed upon time adjustment. As such, inhibition by the arylated product could not account for the reduction in rate. Deuteration studies were consistent with this finding. Treating *N*-Cbz 4-tolyl-pyrrolidine **3b** with 10 mol % $Pd(OAc)_2$ and excess AcOD-d_4 led to deuterium incorporation at *cis*-C(2) and *trans*-C(4), and deuteration also occurred at the *ortho*-positions on the newly installed aromatic ring via a larger 7-membered palladacycle intermediate.[39,59] Despite this, preferential deuteration of substrate **2** was observed when a mixture of **2** and arylated derivative **3b** was treated under the

https://doi.org/10.1021/acscatal.3c01980
ACS Catal. 2023, 13, 9597−9615

same labeling conditions.[60] No difference in reaction rate for the same-excess profile was also observed upon addition of the byproduct KI.[39]

Considering instead irreversible catalyst deactivation, Burés recently reported a VTNA approach to estimate the concentration of the active catalyst in a reaction mixture when direct quantification is not possible.[61] A linear VTNA plot should be expected upon normalization of the timescale for all kinetically active species, but variations in the [active cat.] during the reaction can result in deviation from linearity. As such, mathematic linearization of the VTNA profile provided an indirect way to estimate the [active cat.] at different time points. Here, a nonlinear profile was observed after normalization of the timescale for $[Pd(OAc)_2]$ and [ArI], which exhibited a kinetic order ≠ 0 (Figure 5a). This indicated

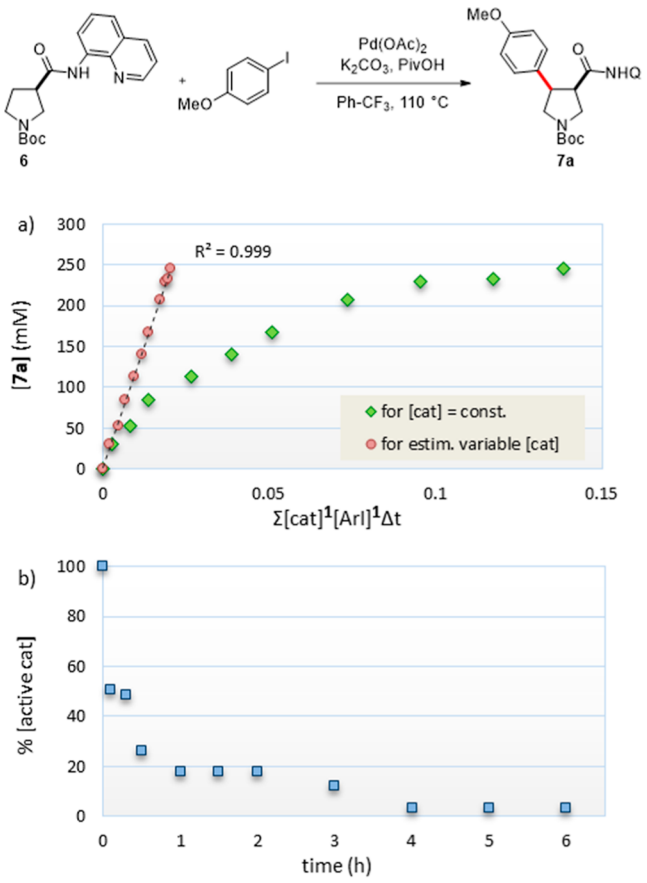

Figure 5. (a) Concentration profiles of **7a** after timescale normalization for all kinetically relevant species. Green diamonds: original VTNA profile assuming [cat.] to be constant during the reaction and equal to the initial $[Pd(OAc)_2]$. Red circles: linearized plot obtained through mathematical estimation of [active cat.]. (b) Estimated profile of catalyst deactivation. Q = quinolin-8-yl.

that the total palladium catalyst concentration was not constant during the reaction. According to Burés' procedure, a series of [cat.] values were calculated to yield a linear VTNA profile (R^2 = 0.999). Plotting the output values as residual active catalyst (%) versus time gave an estimated profile of catalyst deactivation (Figure 5b). This indicated a very fast decrease in active catalyst concentration with <20% remaining after 2 h.

Several plausible causes of catalyst deactivation were evaluated. Reasoning that small amounts of water could form from thermal decomposition of $KHCO_3$,[62,63] the effect of H_2O was first investigated. However, low amounts of water (1−5 equiv) did not affect the reaction.[39]

We then hypothesized that catalyst deactivation could arise from generation of unreactive PdI_2 (Table 1).[64] Despite no

Table 1. Effect of Different Iodide Sources on Catalyst Turnover in the C−H Arylation of Pyrrolidine 6

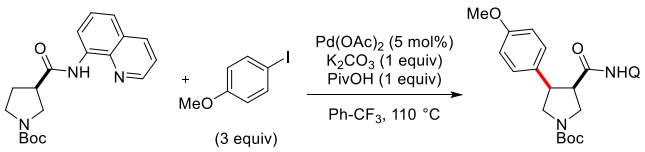

entry	variation from above	**6** (%)[a]	**7a** (%)[a]
1	none	22	67
2	Bu_4NI (1 equiv)	99	
3	KI (1 equiv)	30	62
4	Bu_4NOAc (1 equiv)	99	traces
5	Me_4NCl (1 equiv)	21	61
6	PdI_2 (no K_2CO_3 and PivOH)	99	
7	no K_2CO_3 and PivOH	98	4
8	PdI_2 (no PivOH)	91	7
9	no PivOH	70	28
10	PdI_2	22	64

[a]Determined by ^{1}H NMR using 1,3,5-trimethoxybenzene as the internal standard. Q = quinolin-8-yl.

evidence for KI-mediated inhibition found by RPKA studies,[39] iodides generated in solution during the reaction may be detrimental. In fact, the addition of tetrabutylammonium iodide as a soluble I^- source completely inhibited conversion (entry 2). In contrast, 1 equiv of KI did not affect conversion, likely due to its poor solubility in the reaction media (entry 3). Only traces of the product were found upon addition of Bu_4NOAc, suggesting a detrimental effect of the Bu_4N^+ cation on catalyst turnover presumably through solubilization of iodide (entry 4). On the other hand, using Me_4NCl, which has been reported to form insoluble iodide salts,[64b] did not affect reactivity (entry 5). PdI_2 was not a competent catalyst in the absence of K_2CO_3 and PivOH (entry 6). On the other hand, one turnover was observed using $Pd(OAc)_2$ under the same conditions, giving **7a** in a 4% NMR yield (entry 7). A similar difference between PdI_2 and $Pd(OAc)_2$ was found upon removal of PivOH (entries 8 and 9). Finally, using K_2CO_3 and PivOH in the presence of PdI_2 fully restored catalytic activity (entry 10).

Overall, iodide ions in solution suppressed C−H arylation, likely by formation of unreactive PdI_2.[64] However, the combination of K_2CO_3 and PivOH enabled catalyst turnover, likely by regeneration of CMD-active carboxylate-bound catalytic species and formation of insoluble KI. As such, iodide inhibition is likely to be a cause of catalyst deactivation, particularly at higher conversions. Following similar findings, Wisniewski recently postulated a physical entrapment of the catalyst in a related Pd-catalyzed C(sp^2)−H functionalization with aryl iodides.[65] Catalyst deactivation in our system could be ascribed to a similar effect, although spiking experiments with fresh $Pd(OAc)_2$ did not enable further conversion.[39] Nonetheless, this overall loss of the palladium catalyst was the cause of the incomplete conversion, which limited turnover in our system.

https://doi.org/10.1021/acscatal.3c01980
ACS Catal. 2023, 13, 9597−9615

Scheme 5. Proposed Catalytic Cycle[a]

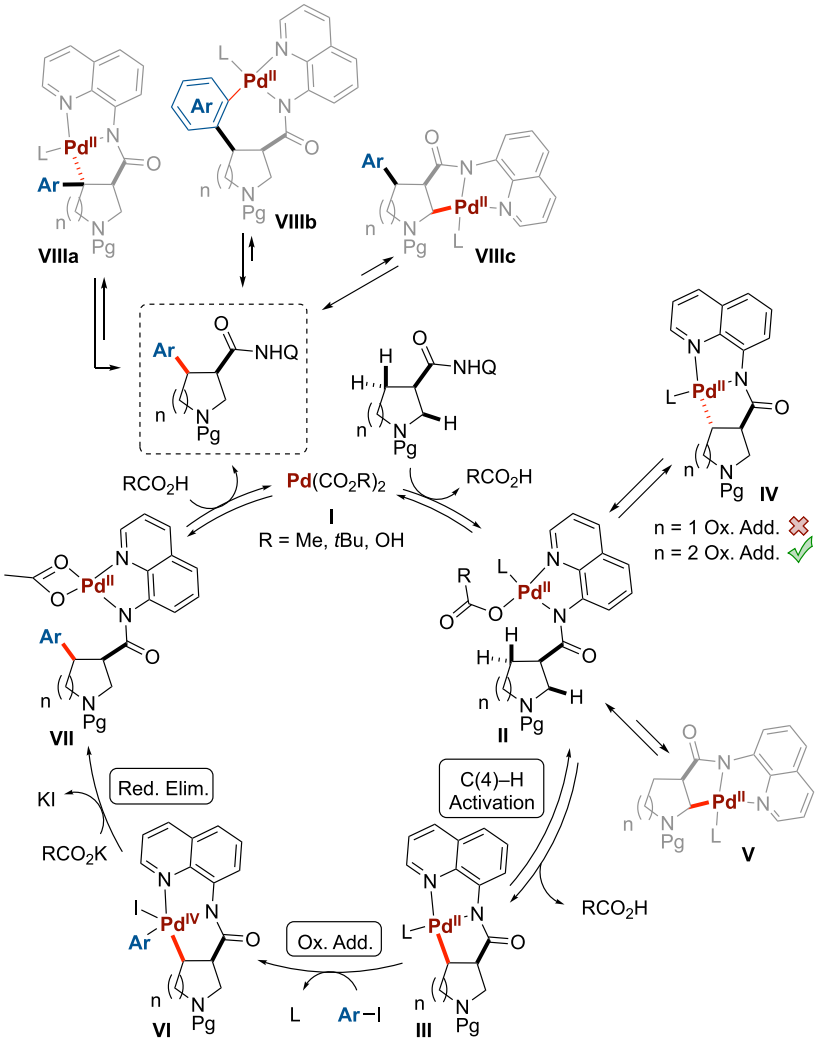

[a]Pg = protecting group. Q = quinolin-8-yl.

Several strategies were investigated to improve reactivity. Ligands were screened in an attempt to stabilize on-cycle Pd species and avoid catalyst deactivation, including monodentate pyridine ligands,[66] monoprotected amino acids, and pyridones which have been shown to promote CMD processes.[67,68] The addition of picolinic acid derivatives was also investigated having been reported by Sanford to avoid catalyst deactivation in the Pd-catalyzed C−H arylation of bicyclic N-heterocycles.[34] However, no improvement in the reaction outcome was observed, nor upon the addition of other additives, including oxidants, halide scavengers, and other coordinating ligands.[39] Switching potassium carbonate to the cesium carbonate, which had been used to circumvent catalyst deactivation deriving from physical entrapment of Pd,[65] did not result in a higher yield of *cis*-C(4)−H arylation but gave higher levels of *cis*-to *trans*-epimerization.[39] Aryl bromides gave very low reactivity (12% conversion). Furthermore, the reaction was unsuccessful with more electrophilic coupling partners, diaryliodonium and aryldiazonium salts, which would have avoided iodide formation.[69] Hence, an alternative approach was required.

Proposed Catalytic Cycle. Based on the above experimental and computational studies, the following Pd^{II}/Pd^{IV} catalytic cycle could be proposed (Scheme 5). Initial catalyst coordination to form intermediate **II** is followed by reversible C−H bond cleavage, proceeding via inner- or outer-sphere CMD. Equally facile cyclometallation can occur at both *cis*- and *trans*-C(4) positions of 5- and 6-membered rings. This in turn gives the corresponding palladacycle complexes **III** and **IV**. Only *cis*-pyrrolidine species **III** can undergo oxidative addition; thus, it is identified as the stereo-determining step for pyrrolidine arylation. On the other hand, the computational analysis indicated a feasible oxidative addition for both diastereomeric piperidine complexes. Deuteration experiments suggested that C−H activation can also occur at *cis*-C(2) from intermediate **II**, though to a lower extent, and very low levels of arylation at C2 are observed.

Formation of Pd(IV) intermediate **VI** after oxidative addition is followed by reductive elimination to forge the new $C(sp^3)-C(sp^2)$ bond. This was identified as the turnover-limiting step, as supported by kinetic analysis and DFT calculations. Finally, halide abstraction and protodemetalation liberate the product and close the catalytic cycle. Importantly, catalyst turnover is enabled by the combination of K_2CO_3 and PivOH, which regenerates the active catalyst while sequestering detrimental iodide as insoluble KI. The arylated product

https://doi.org/10.1021/acscatal.3c01980
ACS Catal. 2023, 13, 9597−9615

Scheme 6. Evaluation of the Steric and Electronic Requirements of the Aminoquinoline Directing group[a]

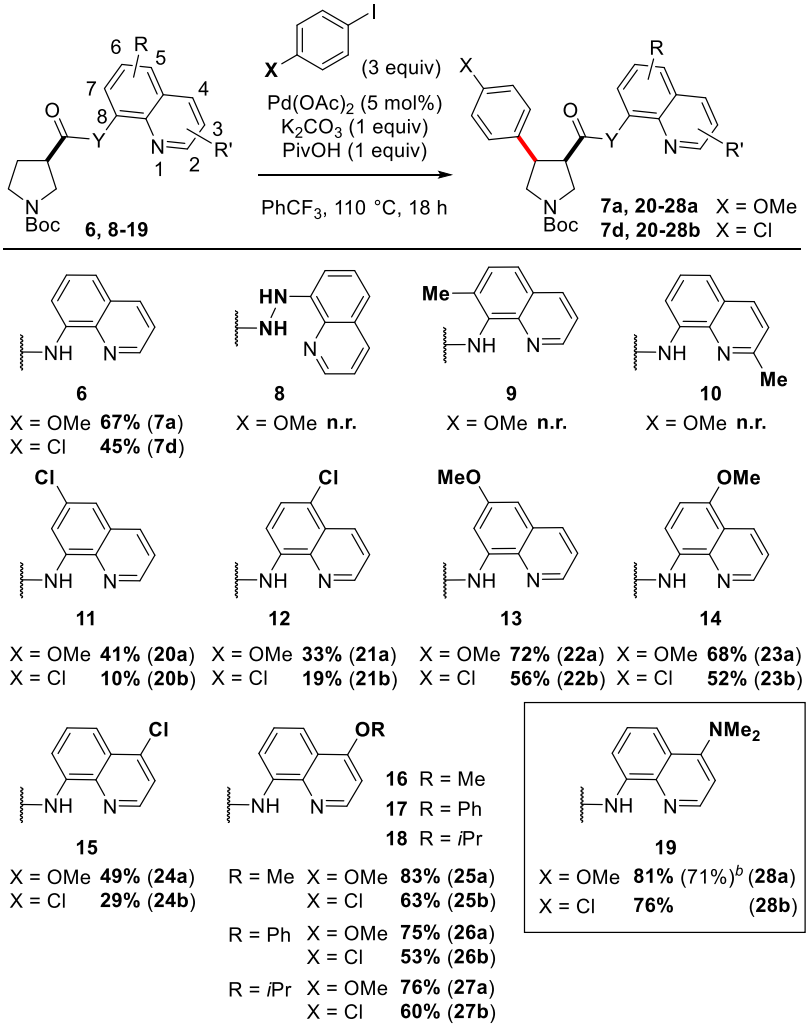

[a]Yields determined by ^{1}H NMR, using 1,3,5-trimethoxybenzene as the internal standard. [b] 1 equiv of ArI was used. n.r. = no reaction.

can also undergo reversible C−H activation forming off-cycle Pd species **VIIIa−c**. Nonetheless, this does not result in catalyst inhibition as confirmed by RPKA studies, likely due to a fast equilibration favoring on-cycle intermediate **III**. On the other hand, VTNA studies showed rapid catalyst deactivation, limiting the efficiency of the reaction. Although a definitive cause could not be identified, it is clear that soluble iodide causes significant inhibition. Subsequent efforts focused on finding a solution to overcome the limitations.

Directing Group Evaluation. As exogenous additives were not successful in improving reactivity, we examined the electronic and steric properties of the aminoquinoline amide directing group. Variations in the pK_a of the proximal (amide NH) or distal (quinoline N) binding sites were anticipated to influence the coordination to the Pd center and impact several elementary steps and off-cycle processes.[70,71] However, the potential to reduce loss of the palladium catalyst was also considered. Factors to improve the reductive elimination step in particular were expected to have a beneficial effect on the reaction efficiency based on the identification of this step as turnover-limiting. To provide insight into the requirements of both coordinating sites of the directing group, we varied both the steric and electronic properties of the aminoquinoline systematically with more electron-rich and electron-poor substituents on both the benzenoid and pyridine rings.[71,72] The substitution of the AQ ring was evaluated in the reaction of pyrrolidine amides with both 4-iodoanisole and 4-chloroiodobenzene to avoid any electronic bias from the coupling partner and aiming to improve the outcome with both (Scheme 6).

First, the use of an acylhydrazide linker (**8**) completely suppressed the reaction, supporting the importance of a 5-membered coordination mode of the directing groups. No reaction was observed upon introduction of a methyl substituent either at the 7- (**9**) or 2-position (**10**) presumably due to unfavorable steric hindrance. Decreasing the electron density on the proximal binding site with a 6-Cl group gave a lower arylation yield (**11**). Similarly, low conversion was observed moving the -Cl substituent to C5 (**12**). Installation of an electron-donating methoxy group in the same positions (**13** and **14**) restored good reactivity, though without any significant improvement from the parent AQ. A similar electronic effect was observed for the distal binding site, with 4-Cl derivative **15** giving lower yields with both aryl iodides. However, a breakthrough in our investigations was obtained in the presence of a methoxy substituent at C4 (**16**). This electron-rich DG afforded *p*-methoxy- and *p*-chlorophenyl pyrrolidine products in 83 and 63% NMR yields, with a 20%

https://doi.org/10.1021/acscatal.3c01980
ACS Catal. 2023, 13, 9597−9615

increase compared to **6**. Encouraged by these promising results, variations in the electron-donating character of the 4-substituent were further explored. Small changes in the ether group did not result in further improvement (**17** and **18**). However, optimal reactivity was finally observed with derivative **19**, bearing a dimethylamino substituent. This DMAQ amide directing group gave the corresponding *p*-chlorophenyl product in a 76% yield, compared to the 45% previously observed. In addition, only a slightly lower NMR yield was found when reducing the loading of 4-iodoanisole to just 1 equiv (71% vs 81%).

Comparison of the reaction profiles for the formation of derivatives **7a** and **28a** showed faster conversion with the new auxiliary, affording the desired product in an 80% yield (by ^{1}H NMR) after just 6 h (Figure 6). This indicated a substantial

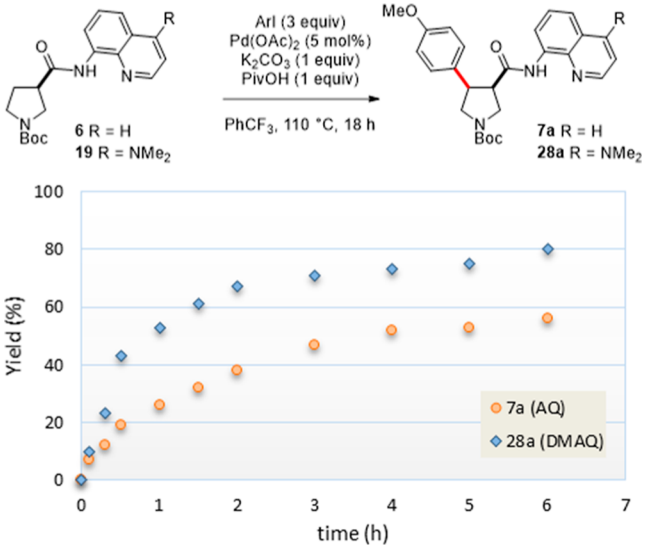

Figure 6. Temporal profiles for C(4)−H arylation with 4-iodoanisole using either AQ or DMAQ directing groups. Yields determined by ^{1}H NMR, using 1,3,5-trimethoxybenzene as the internal standard. Each time point corresponds to a discrete reaction.

improvement in reaction efficiency using DMAQ. It is notable that C4 aminoquinoline substitution is significantly underexplored, and the reaction with **19** represents the first example of this AQ-based directing group used in C−H functionalization.

Kinetic analysis of the reaction using VTNA confirmed a zero-order dependency in pyrrolidine substrate **19**, suggesting no variation in the overall rate law when using the DMAQ auxiliary.[39] However, no significant difference in the estimated catalyst deactivation was found between AQ and DMAQ groups.[39] As such, the effect of different substituents at C4 of the quinoline on the reaction kinetics was investigated to uncover the mechanistic basis for the observed improvement in reactivity. In a competition between substrates **15**−**17** and **19** with unsubstituted AQ amine **6** for a limiting amount of 4-iodoanisole, more electron-rich derivatives showed a preferential reaction. This resulted in a negative Hammett correlation, obtained by plotting $\log([P_X]/[P_H])$ as a function of *para*-substitution constants σ_p (Figure 7a).[50c]

Preferential catalyst coordination to stronger σ-donating DGs may produce a similar observation.[69] Nonetheless, a negative Hammett slope was also found upon analysis of individual arylation rates, suggesting a substitution effect on the turnover-limiting transition state (Figure 7b). Importantly,

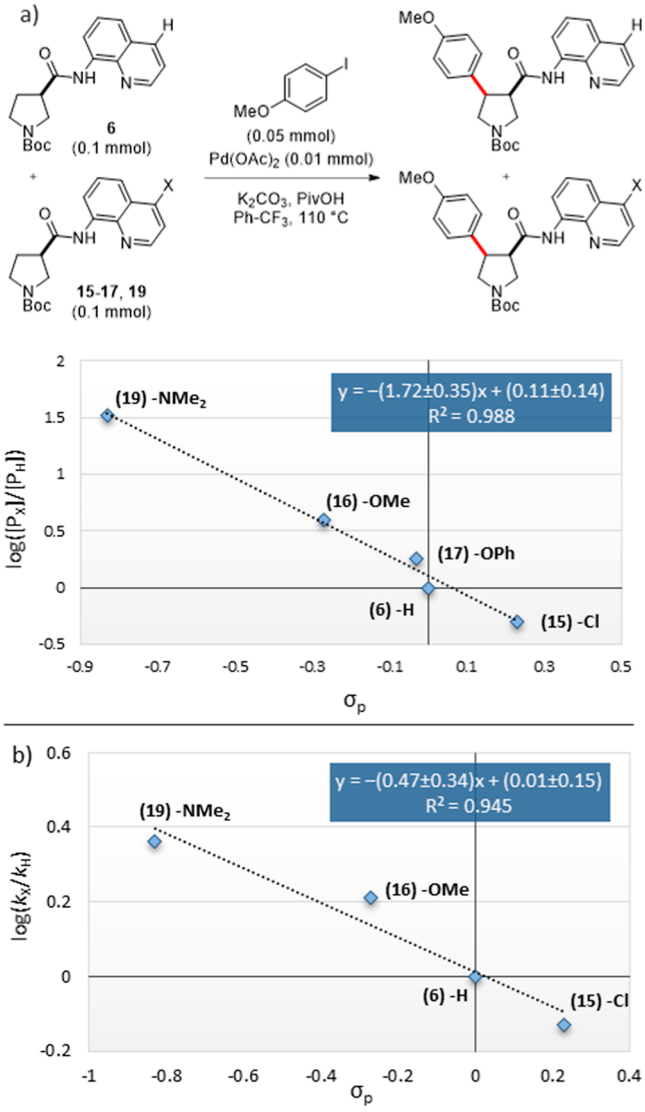

Figure 7. (a) Hammett plot for competition experiments with different 4-substituted quinoline directing groups. (b) Hammett plot of log (k_X/k_H) as a function of σ_p for individual kinetics using different 4-substituted AQ amides.

a >2-fold increase in initial rate was observed using the DMAQ auxiliary (k_{DMAQ} = 6.13 ± 1.01 mM min^{-1} and k_{AQ} = 2.65 ± 0.69 mM min^{-1}).[39] The relatively low k_{DMAQ}/k_{AQ} ratio and hence $\Delta\Delta G^{‡}$ did not afford an appreciable energetic difference for this step by DFT calculations ($\Delta\Delta G_{AQ\text{-}DMAQ}^{‡}$ < 1 kcal mol^{-1}).[39] Nonetheless, this remains significant from a synthetic perspective, leading to the observed improvement. Together, this implies that the DMAQ group provides an advantage to the reductive elimination step.[72,73]

Second-Generation Pyrrolidine and Piperidine C(4)−H Arylation with C3 Directing Groups. With the new DG group in hand, we explored the scope of pyrrolidine C−H arylation (Scheme 7). Pleasingly, the DMAQ auxiliary afforded significantly higher yields of *cis*-3,4-disubstituted pyrrolidine products compared to the first-generation system. Excellent regio- and stereoselectivity were preserved in all cases, with no need to reoptimize the reaction conditions. Furthermore, the higher conversion enabled easier chromatographic purification. *N*-Boc- and *N*-Cbz-protected pyrrolidines **28a** and **30a** were isolated in 78 and 80% yields, respectively. *Para*- and *meta*-

https://doi.org/10.1021/acscatal.3c01980
ACS Catal. 2023, 13, 9597−9615

Scheme 7. Scope of Pyrrolidine C(4)−H Arylation Using a 4-DMAQ Directing Group[a]

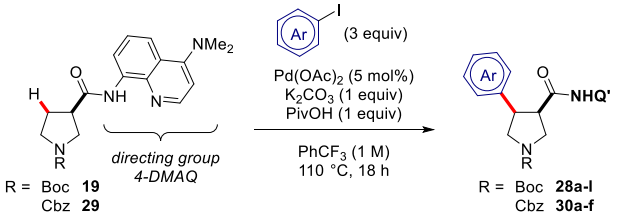

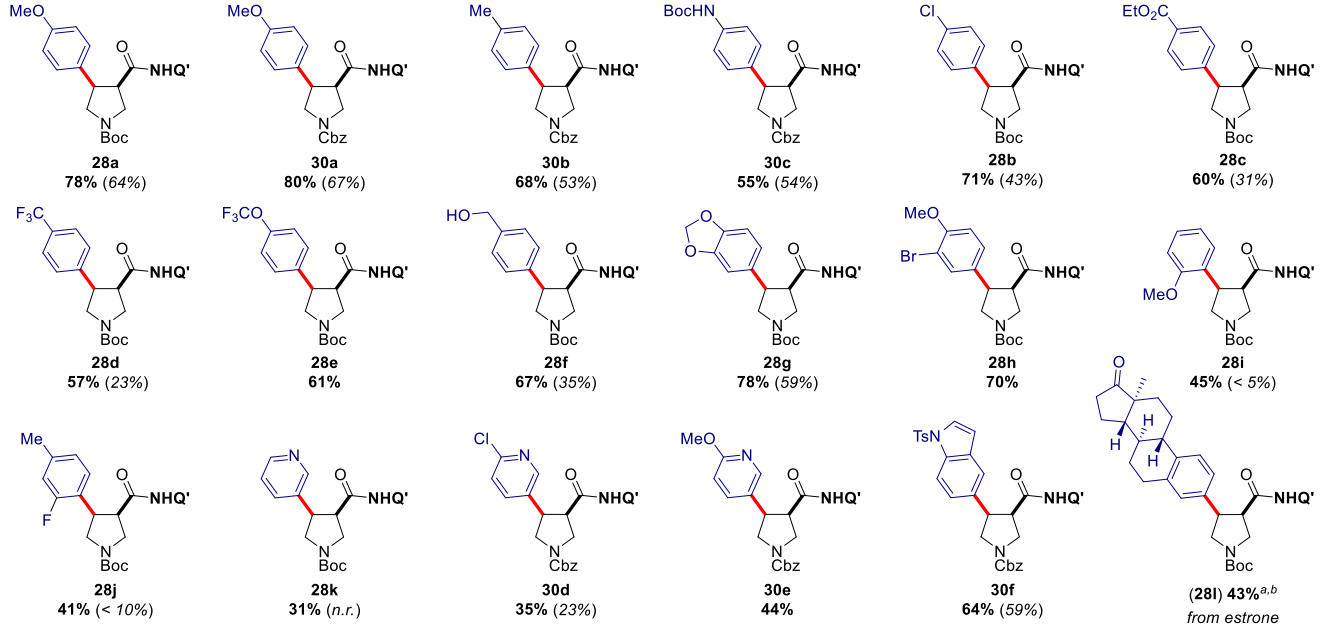

[a]When applicable, yields obtained for the same aryl iodide with the first-generation 8-aminoquinoline system are reported in parenthesis (see ref 35). [a] 1 equiv of ArI used. [b] Isolated as 1:1 mixture of *cis*-3,4-diastereomers. n.r. = no reaction. Q′ = 4-Dimethylamino-quinolin-8-yl.

substituted arenes could be installed in high yields, particularly in the presence of electron-donating substituents (**30b−c** and **28g−h**). The most striking improvements were found in the reaction with more electron-poor aryl iodides. 4-Cl and 4-CO_2Et derivatives **28b** and **28c** were obtained in 71 and 60% yields, respectively, with a ∼30% increase compared to that in the AQ system. Good reactivity was also observed for *p*-trifluoromethyl and *p*-trifluoromethoxy groups, giving 57 and 61% yields of the respective products (**28d−e**). Benzyl alcohol and bromide functionalities were well tolerated, providing useful handles for downstream elaboration (**28f** and **28h**). Pleasingly, the second-generation DMAQ auxiliary allowed the use of *ortho*-substituted aryl iodides. Useful yields were now obtained for *o*-OMe and *o*-F derivatives **28i** and **28j**, which could not be installed using the parent AQ directing group. Importantly, the reaction scope could also be extended to electron-poor heteroaromatic groups. 4-(3-Pyridyl)-pyrrolidine **28k** was isolated in a 31% yield, while no reaction was previously observed. Functionalized pyridines were also tolerated, giving synthetically useful yields of 2-Cl- and 2-OMe-pyridyl derivatives **30d** and **30e**. Good reactivity was observed for *N*-tosyl indole **30f**, formed in a 64% yield. Finally, the new DG could be leveraged to install more complex aromatic substituents. This was exemplified in the synthesis of alkylated estrone derivative **28l**, formed in a 43% yield using just 1 equiv of the valuable estrone-derived iodide. This constitutes a significant improvement in efficiency given that aryl iodides are typically used in significant excess.

Next, we investigated the DMAQ effect on the C−H arylation of piperidine rings. In this case, formation of a small amount of unidentified side products was observed under the same conditions used for pyrrolidines. The reaction with DMAQ facilitated the lowering of the reaction temperature, and optimal results with increased mass balance were obtained at 90 °C.[39] Under these conditions, the second-generation DG provided higher conversion together with an improved *dr* in favor of the *cis*-isomer. This could be again ascribed to an easier reductive elimination, promoting the formation of *cis*-piperidine products (cf. Figure 4). Pleasingly, *cis*-configured *p*-methoxyphenyl piperidine **32a** was formed in a 71% yield, versus 44% with AQ (Scheme 8). Improved yields (58−64%) were also found for paroxetine and Br-paroxetine intermediates **32b** and **32c**.[35,36] Finally, 2-iodothiophene was successfully installed (**32d**), though without any increase in *dr*.

The DMAQ directing group could be efficiently removed using the same conditions previously reported for AQ cleavage.[35] *Cis*- and *trans*-configured carboxylic acid derivatives **33** and **34** were accessed in excellent yield under complementary hydrolytic protocols (Scheme 9). Importantly, the DG could be recovered from the crude reaction mixtures either as the free base or *N*-Boc-protected derivative. Reductive conditions were also demonstrated to afford alcohol-containing pyrrolidine building block **35** in a 69% yield.

The synthetic utility of the improved DMAQ directing group was finally showcased in the late-stage functionalization of bioactive compounds. A two-step functionalization of

https://doi.org/10.1021/acscatal.3c01980
ACS Catal. 2023, 13, 9597−9615

Scheme 8. Piperidine C(4)−H Arylation Using a 4-DMAQ Directing Group[a]

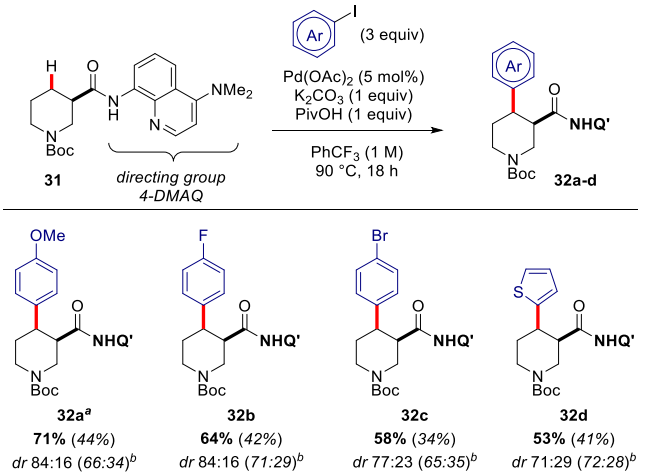

[a]Products isolated as single *cis*-isomers. Yields and *dr* obtained for the same aryl iodide with the first-generation 8-aminoquinoline system are reported in parenthesis (see ref 35). [a] *trans*-diastereomer isolated in a 13% yield. [b] *dr* (*cis*/*trans*) estimated by ^{1}H NMR on the crude reaction mixture. Q′ = 4-dimethylamino-quinolin-8-yl.

Scheme 9. Removal of the 4-DMAQ Directing Group[a]

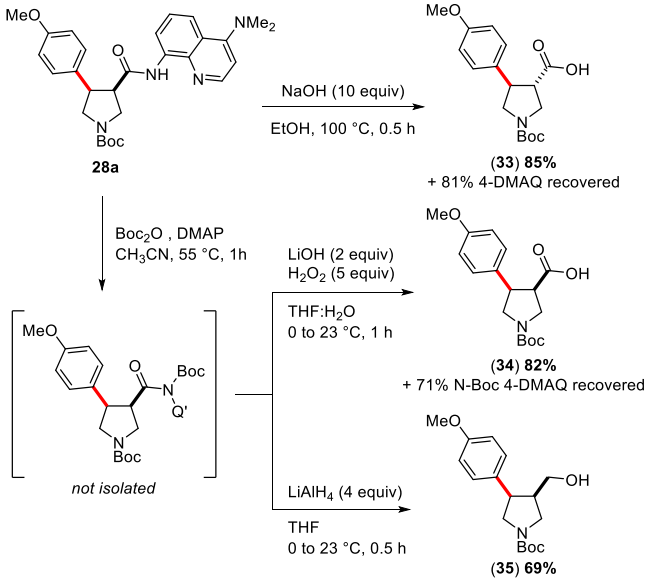

[a]Q′ = 4-dimethylamino-quinolin-8-yl.

benzoic acid derivatives was envisaged to leverage the prevalence of this functional group in drug molecules. We reasoned that decarboxylative iodination followed by DMAQ-enabled C−H arylation would provide expeditious access to N-heterocyclic derivatives of commercial drugs, which would be difficult to access by other means (Scheme 10a). Subsequent directing group removal would regenerate the acid functionality, achieving a formal N-heterocycle insertion into the original pharmacophore. With the possibility to form both *cis*- and *trans*-derivatives upon directing group cleavage, this would offer interesting opportunities for late-stage SAR exploration. First, anti-hyperuricemic probenecid was selected as the model substrate for this study (Scheme 10b).[74]

Scheme 10. Late-Stage Functionalization of Acid-Containing Drugs Enabled by the 4-DMAQ Directing Group; (a) Conceptual Insertion of N-Heterocycles into Arene Carboxylic Acid-Containing Drug Compounds; (b) C−H Functionalization with Probenecid-Derived Aryl Iodide and Directing Group Removal to *cis*- and *trans*-Pyrrolidine Derivatives; (c) C−H Functionalization with Drug-Derived Aryl Iodides[a]

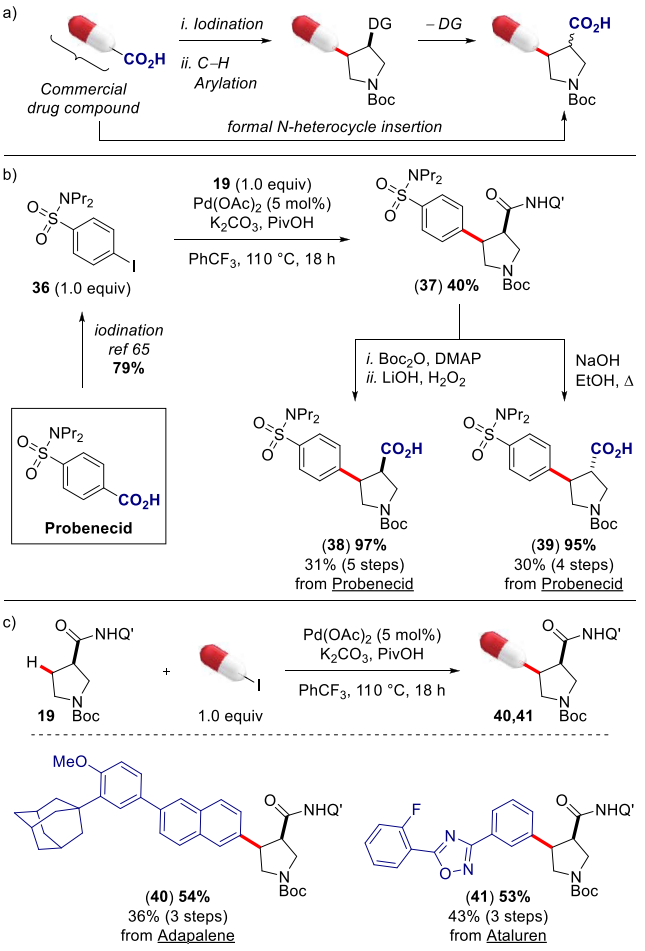

[a]Q′ = 4-dimethylamino-quinolin-8-yl.

Decarboxylative iodination proceeded well using the Pd-catalyzed protocol recently reported by Morandi.[75] Iodide **36** was obtained in a 79% yield and then used in the C(4)−H arylation of pyrrolidine-3-carboxamide **19**. Using just 1 equiv of **36** afforded pyrrolidine derivative **37** in a 40% yield on a 1 mmol scale. A similar transformation would have not been possible using the AQ system, both due to the requirement of 3 equiv of ArI with AQ and the electron-poor character of probenecid iodide **36**. Final removal of the DMAQ directing group afforded *cis*- and *trans*-probenecid derivatives **38** and **39** in nearly quantitative conversion and 30 to 31% yields over 4 to 5 steps from the commercial drug. Pleasingly, adapalene-[76] and ataluren-[77] derived iodides were also successful substrates using 1 equiv of iodide (Scheme 10c). These formed the respective pyrrolidine products **40** and **41** in 54 and 53% yields, highlighting the functional group tolerance of the second-generation C(4)−H arylation protocol.

https://doi.org/10.1021/acscatal.3c01980
ACS Catal. 2023, 13, 9597−9615

CONCLUSIONS

Overall, we have presented mechanistic investigations into the regio- and stereochemical outcome of the C(4)−H arylation of pyrrolidines and piperidines with C3 aminoquinoline amide directing groups. Detailed experimental and computational studies have revealed the significance of the different individual steps on the principal outcomes of the reaction. Key reaction features have been highlighted as follows.

- Deuteration studies indicated that C−H activation, likely occurring through a CMD process, is facile at both *cis*- and *trans*-C4 positions. The rate of deuteration indicates preferential formation of the palladacycle at C4 over C2. In the presence of stabilizing exogenous ligands, the *cis*-C4 palladacycle was isolated. Only a small KIE (k_H/k_D = 1.2) was observed for the CMD step.
- Oxidative addition is the stereo-determining step as revealed by DFT calculations. The *trans*-palladacycle is ∼6 kcal mol^{-1} higher in energy than the *cis*-palladacycle due to increased strain. This energy difference is retained in the oxidative addition transition state, preventing *trans*-arylation in the pyrrolidine series and leading to *cis*-arylated pyrrolidines as single diastereomers. The same reasoning favors the *cis*-product in the piperidines series but with a minor *trans*-product also formed due to a much smaller strain energy difference between *cis*- and *trans*-5,6-fused rings.
- Reductive elimination is the turnover-limiting step for the overall catalytic cycle. Kinetic studies identified first order in ArI and $Pd(OAc)_2$ but zero order in pyrrolidine substrate, suggesting catalyst saturation. Hammett plots displayed a linear dependence with a negative slope, consistent with formation of a partial positive charge in the turnover-limiting reductive elimination. Consequently, the first-generation reaction was less successful with electron-poor aryl iodides.
- K_2CO_3 and PivOH play an important role in enabling catalyst turnover and maintaining a level of catalyst activity in the presence of iodide. Nonetheless, fast catalyst deactivation was observed, limiting overall reaction conversion, likely due to increasing levels of soluble iodide in the reaction.

These mechanistic studies culminated in the development of a novel DMAQ amide directing group. This allowed us to achieve our core synthetic objectives to improve the reaction conversion and yield, as well as to improve the results with electron-poor derivatives. With this removable auxiliary, a >2-fold increase in reaction rate was achieved, forming *cis*-3,4-disubstituted pyrrolidines in 20−30% higher yields compared with the first-generation system. A significant increase in reactivity was obtained with electron-deficient iodoarenes, and the reaction scope could be extended to challenging *ortho*-substituted and heteroaryl iodides that were previously unsuccessful. Increased efficiency was also observed for piperidine rings, together with an improved *cis*-diastereoselectivity. Consequently, a broad scope of aryl iodides was demonstrated. The aryl iodide loading could be reduced to just 1 equiv, enabling the late-stage functionalization of complex natural products and pharmaceuticals. Although slower catalyst deactivation was ruled out, the kinetic analysis suggested stronger coordination to the Pd center and a reduction in the energy required for the turnover-limiting reductive elimination. We envisage that the DMAQ amide will serve as an improved directing group in C−H functionalization reactions, particularly where reductive elimination is turnover-limiting. Further studies to exploit the DMAQ directing group are underway in our laboratories.

ASSOCIATED CONTENT

Supporting Information

The Supporting Information is available free of charge at https://pubs.acs.org/doi/10.1021/acscatal.3c01980.

D-labeling studies; H/D scrambling experiments; KIE studies; reactions with Pd-cycle **4-Py**; VTNA studies with AQ_DG; electronic effects of the ArI and Hammett plot; RPKA; catalyst deactivation studies with AQ; directing group screening; VTNA and catalyst deactivation studies with DMAQ; kinetic effects of different directing groups; diastereoselectivity optimization with piperidine **31**; X-ray structure of **5-PCy$_3$**; additional DFT studies and cartesian coordinates; temperature corrections at 383.15 K; natural charges in C(4)−H arylation of pyrrolidine-3-AQ_amide with IPh; experimental details and characterization data; and NMR data (PDF)

Structure of **5-PCy$_3$** (CIF)

AUTHOR INFORMATION

Corresponding Author

James A. Bull − *Department of Chemistry, Molecular Sciences Research Hub, Imperial College London, London W12 0BZ, U.K.;* orcid.org/0000-0003-3993-5818; Email: j.bull@imperial.ac.uk

Authors

Daniele Antermite − *Department of Chemistry, Molecular Sciences Research Hub, Imperial College London, London W12 0BZ, U.K.*

Andrew J. P. White − *Department of Chemistry, Molecular Sciences Research Hub, Imperial College London, London W12 0BZ, U.K.*

Luis Casarrubios − *Department of Chemistry, Molecular Sciences Research Hub, Imperial College London, London W12 0BZ, U.K.; Departamento de Química Organica I, Facultad de Ciencias Químicas, Universidad Complutense and Centro de Innovación en Química Avanzada (ORFEO−CINQA), Madrid 28040, Spain;* orcid.org/0000-0002-9054-3118

Complete contact information is available at: https://pubs.acs.org/10.1021/acscatal.3c01980

Notes

The authors declare no competing financial interest.

Raw and processed characterization data for all novel compounds can be found at the Imperial College London Research Data Repository: DOI: 10.14469/hpc/11771 https://data.hpc.imperial.ac.uk/resolve/?doi=11771&access=g9kf-9hct.

ACKNOWLEDGMENTS

The authors gratefully acknowledge The Royal Society [University Research Fellowship, UF140161, and URF\R\201019 (to J.A.B.), URF Appointed Grant RG150444 and URF Enhancement Grant RGF\EA\180031]. L.C. gratefully acknowledges the financial support of the Spanish government

for a grant in the 2017 Salvador de Madariaga program. The authors thank the Computing services at Imperial College (HPC) and at the UCM in Madrid (Brigit). They thank Prof. Henry Rzepa for his support and insight into the results of the DFT calculations. They thank Corey Fulop and Peter Haycock for NMR support to obtain the deuteration profiles. They also thank Dr. Alexander Boddy for the preparation of the estrone iodide.

REFERENCES

(1) (a) Yamaguchi, J.; Yamaguchi, A. D.; Itami, K. C−H Bond Functionalization: Emerging Synthetic Tools for Natural Products and Pharmaceuticals. *Angew. Chem., Int. Ed.* **2012**, *51*, 8960−9009. (b) Wencel-Delord, J.; Glorius, F. C−H bond activation enables the rapid construction and late-stage diversification of functional molecules. *Nat. Chem.* **2013**, *5*, 369−375. (c) He, J.; Wasa, M.; Chan, K. S. L.; Shao, Q.; Yu, J.-Q. Palladium-Catalyzed Transformations of Alkyl C−H Bonds. *Chem. Rev.* **2017**, *117*, 8754−8786. (d) Lam, N. Y. S.; Wu, K.; Yu, J.-Q. Advancing the Logic of Chemical Synthesis: C−H Activation as Strategic and Tactical Disconnections for C−C Bond Construction. *Angew. Chem., Int. Ed.* **2021**, *60*, 15767−15790. (e) Dutta, U.; Maiti, S.; Bhattacharya, T.; Maiti, D. Arene diversification through distal C(sp^2)−H functionalization. *Science* **2021**, *372*, No. eabd5992. (f) Guillemard, L.; Kaplaneris, N.; Ackermann, L.; Johansson, M. J. Late-stage C−H functionalization offers new opportunities in drug discovery. *Nat. Rev. Chem.* **2021**, *5*, 522−545. (g) Zhang, L.; Ritter, T. A Perspective on Late-Stage Aromatic C−H Bond Functionalization. *J. Am. Chem. Soc.* **2022**, *144*, 2399−2414.

(2) Vitaku, E.; Smith, D. T.; Njardarson, J. T. Analysis of the Structural Diversity, Substitution Patterns, and Frequency of Nitrogen Heterocycles among U.S. FDA Approved Pharmaceuticals. *J. Med. Chem.* **2014**, *57*, 10257−10274.

(3) (a) Blakemore, D. C.; Castro, L.; Churcher, I.; Rees, D. C.; Thomas, A. W.; Wilson, D. M.; Wood, A. Organic Synthesis Provides Opportunities to Transform Drug Discovery. *Nat. Chem.* **2018**, *10*, 383−394. (b) Campos, K. R.; Coleman, P. J.; Alvarez, J. C.; Dreher, S. D.; Garbaccio, R. M.; Terrett, N. K.; Tillyer, R. D.; Truppo, M. D.; Parmee, E. R. The Importance of Synthetic Chemistry in the Pharmaceutical Industry. *Science* **2019**, *363*, No. eaat0805. (c) Grygorenko, O. O.; Volochnyuk, D. M.; Ryabukhin, S. V.; Judd, D. B. The Symbiotic Relationship Between Drug Discovery and Organic Chemistry. *Chem.—Eur. J.* **2020**, *26*, 1196−1237.

(4) (a) Antermite, D.; Bull, J. A. Transition Metal-Catalyzed Directed C(sp^3)−H Functionalization of Saturated Heterocycles. *Synthesis* **2019**, *51*, 3171−3204. (b) Piticari, A.-S.; Larionova, N.; Bull, J. A. C−H Functionalization of Saturated Heterocycles Beyond the C2 Position. In *Transition-Metal-Catalyzed C-H Functionalization of Heterocycles*; Punniyamurthy, T., Kumar, A., Eds.; Wiley, 2023; pp 567−607.

(5) (a) Caplin, M. J.; Foley, D. J. Emergent Synthetic Methods for the Modular Advancement of sp^3-Rich Fragments. *Chem. Sci.* **2021**, *12*, 4646−4660. (b) Arisawa, M.; Ohno, S.; Miyoshi, M.; Murai, K. Non-Directed β- or γ-C(sp^3)-H Functionalization of Saturated Nitrogen-Containing Heterocycles. *Synthesis* **2021**, *53*, 2947−2960. (c) Chessari, G.; Grainger, R.; Holvey, R. S.; Ludlow, R. F.; Mortenson, P. N.; Rees, D. C. C−H functionalisation tolerant to polar groups could transform fragment-based drug discovery (FBDD). *Chem. Sci.* **2021**, *12*, 11976−11985.

(6) (a) Chen, Z.; Wang, B.; Zhang, J.; Yu, W.; Liu, Z.; Zhang, Y. Transition Metal-Catalyzed C−H Bond Functionalizations by the Use of Diverse Directing Groups. *Org. Chem. Front.* **2015**, *2*, 1107−1295. (b) Sambiagio, C.; Schönbauer, D.; Blieck, R.; Dao-Huy, T.; Pototschnig, G.; Schaaf, P.; Wiesinger, T.; Zia, M. F.; Wencel-Delord, J.; Besset, T.; et al. A Comprehensive Overview of Directing Groups Applied in Metal-Catalysed C-H Functionalisation Chemistry. *Chem. Soc. Rev.* **2018**, *47*, 6603−6743. (c) Rej, S.; Ano, Y.; Chatani, N. Bidentate Directing Groups: An Efficient Tool in C−H Bond Functionalization Chemistry for the Expedient Construction of C−C Bonds. *Chem. Rev.* **2020**, *120*, 1788−1887.

(7) For alternative recent approaches, see: (a) Uttry, A.; Van Gemmeren, M. Direct C(sp^3)−H Activation of Carboxylic Acids. *Synthesis* **2020**, *52*, 479−488. (b) Higham, J. I.; Bull, J. A. Transient Imine Directing Groups for the C−H Functionalisation of Aldehydes, Ketones and Amines: An Update 2018−2020. *Org. Biomol. Chem.* **2020**, *18*, 7291−7315. (c) Sinha, S. K.; Guin, S.; Maiti, S.; Biswas, J. P.; Porey, S.; Maiti, D. Toolbox for Distal C−H Bond Functionalizations in Organic Molecules. *Chem. Rev.* **2022**, *122*, 5682−5841.

(8) (a) Wang, D.-H.; Wasa, M.; Giri, R.; Yu, J.-Q. Pd(II)-Catalyzed Cross-Coupling of sp^3 C−H Bonds with sp^2 and sp^3 Boronic Acids Using Air as the Oxidant. *J. Am. Chem. Soc.* **2008**, *130*, 7190−7191. (b) Wasa, M.; Engle, K. M.; Yu, J.-Q. Pd(0)/PR_3-Catalyzed Intermolecular Arylation of sp^3 C−H Bonds. *J. Am. Chem. Soc.* **2009**, *131*, 9886−9887. (c) Wasa, M.; Chan, K. S. L.; Zhang, X.; He, J.; Miura, M.; Yu, J. Ligand-Enabled Methylene C(sp^3)−H Bond Activation with a Pd(II) Catalyst. *J. Am. Chem. Soc.* **2012**, *134*, 18570−18572. (d) Engle, K. M.; Mei, T.; Wasa, M.; Yu, J.-Q. Weak Coordination as a Powerful Means for Developing Broadly Useful C−H Functionalization Reactions. *Acc. Chem. Res.* **2012**, *45*, 788−802. (e) For early carboxylic acid directed arylation: Giri, R.; Maugel, N.; Li, J. J.; Wang, D. H.; Breazzano, S. P.; Saunders, L. B.; Yu, J.-Q. Palladium-Catalyzed Methylation and Arylation of sp^2 and sp^3 C-H Bonds in Simple Carboxylic Acids. *J. Am. Chem. Soc.* **2007**, *129*, 3510−3511.

(9) (a) Zaitsev, V. G.; Shabashov, D.; Daugulis, O. Highly Regioselective Arylation of sp^3 C−H Bonds Catalyzed by Palladium Acetate. *J. Am. Chem. Soc.* **2005**, *127*, 13154−13155. (b) Shabashov, D.; Daugulis, O. Auxiliary-Assisted Palladium-Catalyzed Arylation and Alkylation of sp^2 and sp^3 Carbon−Hydrogen Bonds. *J. Am. Chem. Soc.* **2010**, *132*, 3965−3972. (c) Tran, L. D.; Daugulis, O. Nonnatural Amino Acid Synthesis by Using Carbon-Hydrogen Bond Functionalization Methodology. *Angew. Chem., Int. Ed.* **2012**, *51*, 5188−5191. (d) Nadres, E. T.; Santos, G. I. F.; Shabashov, D.; Daugulis, O. Scope and Limitations of Auxiliary-Assisted, Palladium-Catalyzed Arylation and Alkylation of sp^2 and sp^3 C−H Bonds. *J. Org. Chem.* **2013**, *78*, 9689−9714. (e) Daugulis, O.; Roane, J.; Tran, L. D. Bidentate, Monoanionic Auxiliary-Directed Functionalization of Carbon-Hydrogen Bonds. *Acc. Chem. Res.* **2015**, *48*, 1053−1064.

(10) (a) Fitzgerald, L. S.; O'Duill, M. L. A Guide to Directing Group Removal: 8-Aminoquinoline. *Chem.—Eur. J.* **2021**, *27*, 8411−8436. (b) Berger, M.; Chauhan, R.; Rodrigues, C. A. B.; Maulide, N. Bridging C−H Activation: Mild and Versatile Cleavage of the 8-Aminoquinoline Directing Group. *Chem.—Eur. J.* **2016**, *22*, 16805−16808. (c) Zhang, Z.; Li, X.; Song, M.; Wan, Y.; Zheng, D.; Zhang, G.; Chen, G. Selective Removal of Aminoquinoline Auxiliary by IBX Oxidation. *J. Org. Chem.* **2019**, *84*, 12792−12799. (d) See also refs 32 and 35.

(11) For selected examples of AQ-directed C−H functionalization using palladium catalysis see: (a) Reddy, B. V. S.; Reddy, L. R.; Corey, E. J. Novel Acetoxylation and C−C Coupling Reactions at Unactivated Positions in α-Amino Acid Derivatives. *Org. Lett.* **2006**, *8*, 3391−3394. (b) Feng, Y.; Chen, G. Total Synthesis of Celogentin C by Stereoselective C−H Activation. *Angew. Chem., Int. Ed.* **2010**, *49*, 958−961. (c) Gutekunst, W. R.; Gianatassio, R.; Baran, P. S. Sequential Csp^3−H Arylation and Olefination: Total Synthesis of the Proposed Structure of Pipercyclobutanamide A. *Angew. Chem., Int. Ed.* **2012**, *51*, 7507−7510. (d) Hoshiya, N.; Kobayashi, T.; Arisawa, M.; Shuto, S. Palladium-Catalyzed Arylation of Cyclopropanes via Directing Group-Mediated C(sp^3)−H Bond Activation To Construct Quaternary Carbon Centers: Synthesis of cis- and trans-1,1,2-Trisubstituted Chiral Cyclopropanes. *Org. Lett.* **2013**, *15*, 6202−6205. (e) Parella, R.; Gopalakrishnan, B.; Babu, S. A. Auxiliary-Enabled Pd-Catalyzed Direct Arylation of Methylene C(sp^3)−H Bond of Cyclopropanes: Highly Diastereoselective Assembling of Di- and Trisubstituted Cyclopropanecarboxamides. *Org. Lett.* **2013**, *15*, 3238−3241. (f) Wang, B.; Nack, W. A.; He, G.; Zhang, S. Y.; Chen,

https://doi.org/10.1021/acscatal.3c01980
ACS Catal. 2023, 13, 9597−9615

G. Palladium-catalyzed trifluoroacetate-promoted mono-arylation of the β-methyl group of alanine at room temperature: synthesis of β-arylated α-amino acids through sequential C−H functionalization. *Chem. Sci.* **2014**, *5*, 3952−3957. (g) Xiong, H.-Y.; Besset, T.; Cahard, D.; Pannecoucke, X. Palladium(II)-Catalyzed Directed Trifluoromethylthiolation of Unactivated C(sp^3)−H Bonds. *J. Org. Chem.* **2015**, *80*, 4204−4212. (h) Chapman, L. M.; Beck, J. C.; Wu, L.; Reisman, S. E. Enantioselective Total Synthesis of (+)-Psiguadial B. *J. Am. Chem. Soc.* **2016**, *138*, 9803−9806. (i) Kinsinger, T.; Kazmaier, U. C−H Functionalization of *N*-Methylated Amino Acids and Peptides as Tool in Natural Product Synthesis: Synthesis of Abyssenine A and Mucronine E. *Org. Lett.* **2018**, *20*, 7726−7730. (j) Zhang, X.; Lu, G.; Sun, M.; Mahankali, M.; Ma, Y.; Zhang, M.; Hua, W.; Hu, Y.; Wang, Q.; Chen, J.; He, G.; Qi, X.; Shen, W.; Liu, P.; Chen, G. A general strategy for synthesis of cyclophane-braced peptide macrocycles via palladium-catalysed intramolecular sp^3 C−H arylation. *Nat. Chem.* **2018**, *10*, 540−548. (k) Beck, J. C.; Lacker, C. R.; Chapman, L. M.; Reisman, S. E. A modular approach to prepare enantioenriched cyclobutanes: synthesis of (+)-rumphellaone A. *Chem. Sci.* **2019**, *10*, 2315−2319.

(12) For selected C−H functionalization examples with other metals, see: (a) Nguyen, T. T.; Grigorjeva, L.; Daugulis, O. Cobalt-Catalyzed, Aminoquinoline-Directed Functionalization of Phosphinic Amide sp^2 C−H Bonds. *ACS Catal.* **2016**, *6*, 551−554. (b) Kanemoto, K.; Horikawa, N.; Hoshino, S.; Tokoro, Y.; Fukuzawa, S. I. Copper-Catalyzed Single C−H Amination of 8-Aminoquinoline-Directed Ferrocenes. *Org. Lett.* **2021**, *23*, 4966−4970. (c) Liu, J.; Yu, L.; Zhuang, S.; Gui, Q.; Chen, X.; Wang, W.; Tan, Z. Copper-Mediated Ortho C−H Sulfonylation of Benzoic Acid Derivatives with Sodium Sulfinates. *Chem. Commun.* **2015**, *51*, 6418−6421. For selected examples with Ni catalysis, see: (d) Aihara, Y.; Chatani, N. Nickel-Catalyzed Direct Alkylation of C−H Bonds in Benzamides and Acrylamides with Functionalized Alkyl Halides via Bidentate-Chelation Assistance. *J. Am. Chem. Soc.* **2013**, *135*, 5308−5311. (e) Aihara, Y.; Chatani, N. Nickel-Catalyzed Direct Arylation of C(sp^3)−H Bonds in Aliphatic Amides via Bidentate-Chelation Assistance. *J. Am. Chem. Soc.* **2014**, *136*, 898−901. (f) Li, M.; Dong, J.; Huang, X.; Li, K.; Wu, Q.; Song, F.; You, J. Nickel-Catalyzed Chelation-Assisted Direct Arylation of Unactivated C(sp^3)−H Bonds with Aryl Halides. *Chem. Commun.* **2014**, *50*, 3944−3946. (g) Xu, S.; Takamatsu, K.; Hirano, K.; Miura, M. Nickel-Catalyzed Stereospecific C−H Coupling of Benzamides with Epoxides. *Angew. Chem., Int. Ed.* **2018**, *57*, 11797−11801.

(13) Aminoquinoline amides have also been applied in alkene functionalization, see: (a) Liu, Z.; Zeng, T.; Yang, K. S.; Engle, K. M. β,γ-Vicinal Dicarbofunctionalization of Alkenyl Carbonyl Compounds via Directed Nucleopalladation. *J. Am. Chem. Soc.* **2016**, *138*, 15122−15125. (b) Derosa, J.; Tran, V. T.; Boulous, M. N.; Chen, J. S.; Engle, K. M. Nickel-Catalyzed β,γ-Dicarbofunctionalization of Alkenyl Carbonyl Compounds via Conjunctive Cross-Coupling. *J. Am. Chem. Soc.* **2017**, *139*, 10657−10660.

(14) (a) See ref 9b. (b) Gutekunst, W. R.; Baran, P. S. Total Synthesis and Structural Revision of the Piperarborenines via Sequential Cyclobutane C−H Arylation. *J. Am. Chem. Soc.* **2011**, *133*, 19076−19079.

(15) (a) Chen, F. J.; Zhao, S.; Hu, F.; Chen, K.; Zhang, Q.; Zhang, S. Q.; Shi, B. F. Pd(II)-Catalyzed Alkoxylation of Unactivated C(sp^3)−H and C(sp^2)−H Bonds Using a Removable Directing Group: Efficient Synthesis of Alkyl Ethers. *Chem. Sci.* **2013**, *4*, 4187−4192. (b) Zhang, Q.; Chen, K.; Rao, W.; Zhang, Y.; Chen, F. J.; Shi, B. F. Stereoselective Synthesis of Chiral α-Amino-β-Lactams through Palladium(II)-Catalyzed Sequential Monoarylation/Amidation of C(sp^3)-H Bonds. *Angew. Chem., Int. Ed.* **2013**, *52*, 13588−13592. (c) Zhang, Q.; Yin, X.-S.; Zhao, S.; Fang, S.-L.; Shi, B.-F. Pd(II)-Catalyzed Arylation of Unactivated Methylene C(sp^3)−H Bonds with Aryl Halides Using a Removable Auxiliary. *Chem. Commun.* **2014**, *50*, 8353−8355. (d) Zhang, Q.; Shi, B. F. 2-(Pyridin-2-yl)Isopropyl (PIP) Amine: An Enabling Directing Group for Divergent and Asymmetric Functionalization of Unactivated Methylene C(sp^3)-H Bonds. *Acc. Chem. Res.* **2021**, *54*, 2750−2763.

(16) For other leading examples of bidentate directing groups, see: (a) Jerhaoui, S.; Chahdoura, F.; Rose, C.; Djukic, J.-P.; Wencel-Delord, J.; Colobert, F. Enantiopure Sulfinyl Aniline as a Removable and Recyclable Chiral Auxiliary for Asymmetric C(sp^3)−H Bond Activation. *Chem.—Eur. J.* **2016**, *22*, 17397−17406. (b) Zhang, Y.-F.; Zhao, H.-W.; Wang, H.; Wei, J.-B.; Shi, Z.-J. Readily Removable Directing Group Assisted Chemo- and Regioselective C(sp^3)−H Activation by Palladium Catalysis. *Angew. Chem., Int. Ed.* **2015**, *54*, 13686−13690. (c) Rit, R. K.; Yadav, M. R.; Sahoo, A. K. Pd(II)-Catalyzed Primary-C(sp^3)−H Acyloxylation at Room Temperature. *Org. Lett.* **2012**, *14*, 3724−3727.

(17) He, G.; Zhang, S.-Y.; Nack, W.; Li, Q.; Chen, G. Use of a Readily Removable Auxiliary Group for the Synthesis of Pyrrolidones by the Palladium-Catalyzed Intramolecular Amination of Unactivated γ C(sp^3)-H Bonds. *Angew. Chem., Int. Ed.* **2013**, *52*, 11124−11128.

(18) (a) Tong, H.-R.; Zheng, S.; Li, X.; Deng, Z.; Wang, H.; He, G.; Peng, Q.; Chen, G. Pd(0)-Catalyzed Bidentate Auxiliary Directed Enantioselective Benzylic C−H Arylation of 3-Arylpropanamides Using the BINOL Phosphoramidite Ligand. *ACS Catal.* **2018**, *8*, 11502−11512. (b) Tong, H.-R.; Zheng, W.; Lv, X.; He, G.; Liu, P.; Chen, G. Asymmetric Synthesis of β-Lactam via Palladium-Catalyzed Enantioselective Intramolecular C(sp^3)−H Amidation. *ACS Catal.* **2020**, *10*, 114−120.

(19) Aminoquinoline substitution has also been used to avoid competing C5-functionalization. See: (a) Yang, X.; Sun, Y.; Sun, T.; Rao, Y. Auxiliary-assisted palladium-catalyzed halogenation of unactivated C(sp^3)−H bonds at room temperature. *Chem. Commun.* **2016**, *52*, 6423−6426. (b) Zhao, Q.; Chen, M.-Y.; Poisson, T.; Pannecoucke, X.; Bouillon, J.-P.; Besset, T. Pd-Catalyzed Trifluoromethylthiolation of Unsaturated Compounds: A General Approach. *Eur. J. Org. Chem.* **2018**, *2018*, 6167−6175. (c) Also see: Kim, Y. B.; Won, J.; Lee, J.; Kim, J.; Zhou, B.; Park, J. W.; Baik, M. H.; Chang, S. Ni-Catalyzed Intermolecular C(sp^3)-H Amidation Tuned by Bidentate Directing Groups. *ACS Catal.* **2021**, *11*, 3067−3072.

(20) For the isolation of an aryl-Pd(IV)-complex, see: (a) Vicente, J.; Arcas, A.; Juliá-Hernández, F.; Bautista, D. Synthesis of a Palladium(IV) Complex by Oxidative Addition of an Aryl Halide to Palladium(II) and Its Use as Precatalyst in a C−C Coupling Reaction. *Angew. Chem., Int. Ed.* **2011**, *50*, 6896−6899. (b) See also ref 9b.

(21) For selected mechanistic studies on C−C and C−heteroatom bond-forming reductive elimination from Pd(IV) complexes, see: (a) Racowski, J. M.; Dick, A. R.; Sanford, M. S. Detailed Study of C−O and C−C Bond-Forming Reductive Elimination from Stable $C_2N_2O_2$−Ligated Palladium(IV) Complexes. *J. Am. Chem. Soc.* **2009**, *131*, 10974−10983. (b) Furuya, T.; Benitez, D.; Tkatchouk, E.; Strom, A. E.; Tang, P.; Goddard, W. A.; Ritter, T. Mechanism of C−F Reductive Elimination from Palladium(IV) Fluorides. *J. Am. Chem. Soc.* **2010**, *132*, 3793−3807. (c) Ball, N. D.; Kampf, J. W.; Sanford, M. S. Aryl−CF_3 Bond-Forming Reductive Elimination from Palladium(IV). *J. Am. Chem. Soc.* **2010**, *132*, 2878−2879. (d) Camasso, N. M.; Pérez-Temprano, M. H.; Sanford, M. S. C(sp^3)−O Bond-Forming Reductive Elimination from Pd^{IV} with Diverse Oxygen Nucleophiles. *J. Am. Chem. Soc.* **2014**, *136*, 12771−12775.

(22) For selected reviews on the CMD mechanism, see: (a) Lapointe, D.; Fagnou, K. Overview of the Mechanistic Work on the Concerted Metallation−Deprotonation Pathway. *Chem. Lett.* **2010**, *39*, 1118−1126. (b) Ackermann, L. Carboxylate-Assisted Transition-Metal-Catalyzed C−H Bond Functionalizations: Mechanism and Scope. *Chem. Rev.* **2011**, *111*, 1315−1345. (c) Davies, D. L.; Macgregor, S. A.; McMullin, C. L. Computational Studies of Carboxylate-Assisted C−H Activation and Functionalization at Group 8−10 Transition Metal Centers. *Chem. Rev.* **2017**, *117*, 8649−8709. (d) Altus, K. M.; Love, J. A. The Continuum of Carbon−Hydrogen (C−H) Activation Mechanisms and Terminology. *Commun. Chem.* **2021**, *4*, 173.

(23) For selected studies indicating turnover-limiting C−H activation, see: (a) Yan, S.-B.; Zhang, S.; Duan, W.-L. Palladium-

https://doi.org/10.1021/acscatal.3c01980
ACS Catal. 2023, 13, 9597−9615

Catalyzed Asymmetric Arylation of C(sp^3)−H Bonds of Aliphatic Amides: Controlling Enantioselectivity Using Chiral Phosphoric Amides/Acids. *Org. Lett.* **2015**, *17*, 2458−2461. (b) Dewyer, A. L.; Zimmerman, P. M. Simulated Mechanism for Palladium-Catalyzed, Directed γ-Arylation of Piperidine. *ACS Catal.* **2017**, *7*, 5466−5477. (c) Plata, R. E.; Hill, D. E.; Haines, B. E.; Musaev, D. G.; Chu, L.; Hickey, D. P.; Sigman, M. S.; Yu, J.-Q.; Blackmond, D. G. A Role for Pd(IV) in Catalytic Enantioselective C−H Functionalization with Monoprotected Amino Acid Ligands under Mild Conditions. *J. Am. Chem. Soc.* **2017**, *139*, 9238−9245. (d) Yang, Y.-F.; Chen, G.; Hong, X.; Yu, J.-Q.; Houk, K. N. The Origins of Dramatic Differences in Five-Membered vs Six-Membered Chelation of Pd(II) on Efficiency of C(sp^3)−H Bond Activation. *J. Am. Chem. Soc.* **2017**, *139*, 8514−8521. (e) Sun, Q.; Zhang, H.; Wang, Q.; Qiao, T.; He, G.; Chen, G. Stereoselective Synthesis of C-Vinyl Glycosides via Palladium-Catalyzed C−H Glycosylation of Alkenes. *Angew. Chem., Int. Ed.* **2021**, *60*, 19620−19625.

(24) For an example of turnover-limiting oxidative addition in directed C−H arylation, see: Wei, Y.; Tang, H.; Cong, X.; Rao, B.; Wu, C.; Zeng, X. Pd(II)-Catalyzed Intermolecular Arylation of Unactivated C(sp^3)−H Bonds with Aryl Bromides Enabled by 8-Aminoquinoline Auxiliary. *Org. Lett.* **2014**, *16*, 2248−2251.

(25) For selected examples of C−X bond forming C−H functionalization controlled by reductive elimination, see: (a) He, G.; Lu, G.; Guo, Z.; Liu, P.; Chen, G. Benzazetidine synthesis via palladium-catalysed intramolecular C−H amination. *Nat. Chem.* **2016**, *8*, 1131−1136. (b) Park, H.; Verma, P.; Hong, K.; Yu, J.-Q. Controlling Pd(iv) reductive elimination pathways enables Pd(ii)-catalysed enantioselective C(sp^3)−H fluorination. *Nat. Chem.* **2018**, *10*, 755−762. (c) Nappi, M.; He, C.; Whitehurst, W. G.; Chappell, B. G. N.; Gaunt, M. J. Selective Reductive Elimination at Alkyl Palladium(IV) by Dissociative Ligand Ionization: Catalytic C(sp^3)−H Amination to Azetidines. *Angew. Chem., Int. Ed.* **2018**, *57*, 3178−3182. (d) For an example of turnover-limiting reductive elimination in directed C−H arylation, see ref 18a.

(26) Affron, D. P.; Davis, O. A.; Bull, J. A. Regio- and Stereospecific Synthesis of C-3 Functionalized Proline Derivatives by Palladium Catalyzed Directed C(sp^3)−H Arylation. *Org. Lett.* **2014**, *16*, 4956−4959.

(27) (a) Affron, D. P.; Bull, J. A. Palladium-Catalyzed Directed C(sp^3)-H Arylation of Saturated Heterocycles at C-3 Using a Concise Optimization Approach. *Eur. J. Org. Chem.* **2016**, *2016*, 139−149. (b) Ye, S.; Yang, W.; Coon, T.; Fanning, D.; Neubert, T.; Stamos, D.; Yu, J.-Q. N-Heterocyclic Carbene Ligand-Enabled C(sp^3)−H Arylation of Piperidine and Tetrahydropyran Derivatives. *Chem.—Eur. J.* **2016**, *22*, 4748−4752. (c) Yu, Q.-Y.; Zhong, H.-M.; Sun, W.-W.; Zhang, S.-J.; Cao, P.; Dong, X.-P.; Qin, H.-B.; Liu, J.-K.; Wu, B. Palladium-Catalyzed C(sp^3)−H Functionalization at the C3 Position of L-Pipecolinic Acid Derivatives. *Asian J. Org. Chem.* **2016**, *5*, 608−612.

(28) Maetani, M.; Zoller, J.; Melillo, B.; Verho, O.; Kato, N.; Pu, J.; Comer, E.; Schreiber, S. L. Synthesis of a Bicyclic Azetidine with In Vivo Antimalarial Activity Enabled by Stereospecific, Directed C(sp^3)−H Arylation. *J. Am. Chem. Soc.* **2017**, *139*, 11300−11306.

(29) (a) Hutskalova, V.; Mykhailiuk, P. K. Pd-Catalyzed directed*CH*-(hetero)arylation of cyclic α-amino acids: effects of substituents and the ring size. *Org. Biomol. Chem.* **2019**, *17*, 4342−4349. (b) Also see: Shang, M.; Feu, K. S.; Vantourout, J. C.; Barton, L. M.; Osswald, H. L.; Kato, N.; Gagaring, K.; McNamara, C. W.; Chen, G.; Hu, L.; et al. Modular, stereocontrolled C_β−H/C_α−C activation of alkyl carboxylic acids. *Proc. Natl. Acad. Sci.* **2019**, *116*, 8721−8727.

(30) For examples of O-heterocycles, see: (a) Parella, R.; Babu, S. A. Regio- and Stereoselective Pd-Catalyzed Direct Arylation of Unactivated sp^3 C(3)−H Bonds of Tetrahydrofuran and 1,4-Benzodioxane Systems. *J. Org. Chem.* **2015**, *80*, 2339−2355. Also see refs 27a, 32

(31) Van Steijvoort, B. F.; Kaval, N.; Kulago, A. A.; Maes, B. U. W. Remote Functionalization: Palladium-Catalyzed C5(sp^3)-H Arylation of 1-Boc-3-Aminopiperidine through the Use of a Bidentate Directing Group. *ACS Catal.* **2016**, *6*, 4486−4490.

(32) Piticari, A.-S.; Antermite, D.; Higham, J. I.; Moore, J. H.; Webster, M. P.; Bull, J. A. Stereoselective Palladium-Catalyzed C(sp^3)−H Mono-Arylation of Piperidines and Tetrahydropyrans with a C(4) Directing Group. *Adv. Synth. Catal.* **2022**, *364*, 1488−1497.

(33) (a) Topczewski, J. J.; Cabrera, P. J.; Saper, N. I.; Sanford, M. S. Palladium-Catalysed Transannular C−H Functionalization of Alicyclic Amines. *Nature* **2016**, *531*, 220−224. (b) Aguilera, E. Y.; Sanford, M. S. Model Complexes for the Palladium-Catalyzed Transannular C−H Functionalization of Alicyclic Amines. *Organometallics* **2019**, *38*, 138−142.

(34) Cabrera, P. J.; Lee, M.; Sanford, M. S. Second-Generation Palladium Catalyst System for Transannular C−H Functionalization of Azabicycloalkanes. *J. Am. Chem. Soc.* **2018**, *140*, 5599−5606.

(35) Antermite, D.; Affron, D. P.; Bull, J. A. Regio- and Stereoselective Palladium-Catalyzed C(sp^3)−H Arylation of Pyrrolidines and Piperidines with C(3) Directing Groups. *Org. Lett.* **2018**, *20*, 3948−3952.

(36) Coleman, J. A.; Navratna, V.; Antermite, D.; Yang, D.; Bull, J. A.; Gouaux, E. Chemical and structural investigation of the paroxetine-human serotonin transporter complex. *eLife* **2020**, *9*, No. e56427.

(37) Cbz is used in preference to Boc to avoid potential deprotection under acetic acid conditions.

(38) Yang, X.; Sun, T.-Y.; Rao, Y. A Preliminary Study of Diastereoselectivity in the Pd^{II}-Catalyzed C(sp^3)−H Alkoxylation of Cyclic Systems. *Chem.—Eur. J.* **2016**, *22*, 3273−3277.

(39) See the Supporting Information for full details.

(40) (a) Probst, N. P.; Grelier, G.; Dahaoui, S.; Alami, M.; Gandon, V.; Messaoudi, S. Palladium(II)-Catalyzed Diastereoselective 2,3-*trans* C(sp^3)−H Arylation of Glycosides. *ACS Catal.* **2018**, *8*, 7781−7786. (b) Also see ref 27a.

(41) For selected reviews, see: (a) Gant, T. G. Using Deuterium in Drug Discovery: Leaving the Label in the Drug. *J. Med. Chem.* **2014**, *57*, 3595−3611. (b) Atzrodt, J.; Derdau, V.; Kerr, W. J.; Reid, M. Deuterium- and Tritium-I Compounds: Applications in the Life Sciences. *Angew. Chem., Int. Ed.* **2018**, *57*, 1758−1784. (c) Pirali, T.; Serafini, M.; Cargnin, S.; Genazzani, A. A. Applications of Deuterium in Medicinal Chemistry. *J. Med. Chem.* **2019**, *62*, 5276−5297. (d) Prakash, G.; Paul, N.; Oliver, G. A.; Werz, D. B.; Maiti, D. C−H deuteration of organic compounds and potential drug candidates. *Chem. Soc. Rev.* **2022**, *51*, 3123−3163. Also see: (e) Farizyan, M.; Mondal, A.; Mal, S.; Deufel, F.; Van Gemmeren, M. Palladium-Catalyzed Nondirected Late-Stage C-H Deuteration of Arenes. *J. Am. Chem. Soc.* **2021**, *143*, 16370−16376. (f) Uttry, A.; Mal, S.; van Gemmeren, M. Late-Stage β-C(sp^3)−H Deuteration of Carboxylic Acids. *J. Am. Chem. Soc.* **2021**, *143*, 10895−10901.

(42) An isotopic profile consistent with bis- (18.4%) and tris-deuteration (81.6%) was determined for **2-d_3** by HRMS.

(43) Simmons, E. M.; Hartwig, J. F. On the Interpretation of Deuterium Kinetic Isotope Effects in C−H Bond Functionalizations by Transition-Metal Complexes. *Angew. Chem., Int. Ed.* **2012**, *51*, 3066−3072.

(44) (a) Burés, J. A Simple Graphical Method to Determine the Order in Catalyst. *Angew. Chem., Int. Ed.* **2016**, *55*, 2028−2031. (b) Burés, J. Variable Time Normalization Analysis: General Graphical Elucidation of Reaction Orders from Concentration Profiles. *Angew. Chem., Int. Ed.* **2016**, *55*, 16084−16087. (c) Nielsen, C. D. T.; Burés, J. Visual kinetic analysis. *Chem. Sci.* **2019**, *10*, 348−353.

(45) Attempts to isolate **I-1** or related complexes were unsuccessful under various conditions. The reaction of **2** with stoichiometric $Pd(OAc)_2$ or $Pd(OPiv)_2$, with or without external KOPiv in different solvents, only yielded complex mixtures that could not be definitively isolated or characterized, while addition of pyridine only formed **4-Py**. Furthermore, no Pd(II) complex was observed by in situ NMR in d_4-

https://doi.org/10.1021/acscatal.3c01980
ACS Catal. 2023, 13, 9597−9615

acetic acid, with exclusive formation of the deuterated pyrrolidine derivative.

(46) (a) Fitton, P.; Rick, E. A. The addition of aryl halides to tetrakis(triphenylphosphine)palladium(0). *J. Organomet. Chem.* **1971**, *28*, 287−291. (b) Fauvarque, J. F.; Pflüger, F.; Troupel, M. Kinetics of oxidative addition of zerovalent palladium to aromatic iodides. *J. Organomet. Chem.* **1981**, *208*, 419−427. (c) Surry, D. S.; Buchwald, S. L. Dialkylbiaryl Phosphines in Pd-Catalyzed Amination: A User's Guide. *Chem. Sci.* **2011**, *2*, 27−50.

(47) Oxidative addition is a formal reduction of the aryl iodide and is commonly perceived to be more facile with electron-poor substrates. Conversely, the reductive elimination step is a formal oxidation of the two reacting carbon centers.

(48) For studies on reductive elimination from Pd(IV), see: (a) Canty, A. J.; Watson, A. A.; Skelton, B. W.; White, A. H. Studies of Oxidative Addition-Reductive Elimination Reactions, and the Crystal Structure of the Palladium(IV) Complex Me_2(p-$BrC_6H_4CH_2$)Pd(Phen)Br. *J. Organomet. Chem.* **1989**, *367*, C25−C28. (b) Sharma, M.; Ariafard, A.; Canty, A. J.; Yates, B. F.; Gardiner, M. G.; Jones, R. C. Synthetic and Computational Studies of the Palladium(Iv) System Pd(Alkyl)(Aryl)(Alkynyl)(Bidentate)(Triflate) Exhibiting Selectivity in C−C Reductive Elimination. *Dalton Trans.* **2012**, *41*, 11820−11828.

(49) Sehnal, P.; Taylor, R. J. K.; Fairlamb, I. J. S. Emergence of Palladium(IV) Chemistry in Synthesis and Catalysis. *Chem. Rev.* **2010**, *110*, 824−889.

(50) (a) Hammett, L. P. The Effect of Structure upon the Reactions of Organic Compounds. Benzene Derivatives. *J. Am. Chem. Soc.* **1937**, *59*, 96−103. (b) Brown, H. C.; Okamoto, Y. Electrophilic Substituent Constants. *J. Am. Chem. Soc.* **1958**, *80*, 4979−4987. (c) Hansch, C.; Leo, A.; Taft, R. W. A survey of Hammett substituent constants and resonance and field parameters. *Chem. Rev.* **1991**, *91*, 165−195.

(51) The *N*-Moc protecting group was shown to perform the same as *N*-Boc experimentally, both in C−H arylation and C−H deuteration reactions. The arylation reaction is also productive in toluene as a solvent. See the Supporting Information and ref 35 for further details.

(52) Zhang, B.-S.; Li, Y.; An, Y.; Zhang, Z.; Liu, C.; Wang, X.-G.; Liang, Y.-M. Carboxylate Ligand-Exchanged Amination/C(sp^3)−H Arylation Reaction via Pd/Norbornene Cooperative Catalysis. *ACS Catal.* **2018**, *8*, 11827−11833.

(53) Coomber, C. E.; Benhamou, L.; Bučar, D. K.; Smith, P. D.; Porter, M. J.; Sheppard, T. D. Silver-Free Palladium-Catalyzed C(sp^3)−H Arylation of Saturated Bicyclic Amine Scaffolds. *J. Org. Chem.* **2018**, *83*, 2495−2503.

(54) In carbocyclic fused 5,5-rings, the *trans*-configuration is approximately 6 kcal mol^{-1} less stable than the *cis*-configuration. By comparison, the carbocyclic fused 6,5-series has only a 1 kcal/mol difference between *cis*- and *trans*-configurations. (a) See: Chang, S.-J.; McNally, D.; Shary-Tehrany, S.; Hickey, M. J.; Boyd, R. H. Heats of Combustion and Strain Energies of Bicyclo[n.m.o]Alkanes. *J. Am. Chem. Soc.* **1970**, *92*, 3109−3118. (b) For further discussion and a synthetic example in the carbocyclic series, see: Jamison, T. F.; Shambayati, S.; Crowe, W. E.; Schreiber, S. L. Tandem Use of Cobalt-Mediated Reactions to Synthesize (+)-Epoxydictymene, a Diterpene Containing a Trans-Fused 5−5 Ring System. *J. Am. Chem. Soc.* **1997**, *119*, 4353−4363. The values for the, albeit simpler, carbocyclic fused ring systems are consistent with the values observed in the palladacycles. These considerations correspond to a higher strain energy in the pyrrolidine palladacycle series than in the piperidine series. The energy in the piperidine series leads to more similar maximum transition state energies (for *cis*- and *trans*-arylation) and to lower diastereoselectivity than for the pyrrolidine series

(55) Liu, J.-B.; Tian, Y.-Y.; Zhang, X.; Wang, L.-L.; Chen, D.-Z. A computational mechanistic study of Pd(ii)-catalyzed γ-C(sp^3)−H olefination/cyclization of amines: the roles of bicarbonate and ligand effect. *Dalton Trans.* **2018**, *47*, 4893−4901.

(56) Selectivity of the oxidative addition and reductive elimination steps did not show significant changes when calculated at T = 383.15 K at the same level of theory. See the Supporting Information for further details.

(57) Nucleophilic substitution, SET, atom transfer, and σ-bond metathesis were considered as possible alternatives to the classical oxidative addition step and were investigated computationally. However, all attempts to locate the corresponding transition structures were fruitless. See, (a) Jones, G. O.; Liu, P.; Houk, K. N.; Buchwald, S. L. Computational Explorations of Mechanisms and Ligand-Directed Selectivities of Copper-Catalyzed Ullmann-Type Reactions. *J. Am. Chem. Soc.* **2010**, *132*, 6205−6213. (b) Besora, M.; Maseras, F. The diverse mechanisms for the oxidative addition of C−Br bonds to Pd(PR_3) and Pd(PR_3)$_2$ complexes. *Dalton Trans.* **2019**, *48*, 16242−16248.

(58) (a) Blackmond, D. G. Reaction Progress Kinetic Analysis: A Powerful Methodology for Mechanistic Studies of Complex Catalytic Reactions. *Angew. Chem., Int. Ed.* **2005**, *44*, 4302−4320. (b) Baxter, R. D.; Sale, D.; Engle, K. M.; Yu, J.-Q.; Blackmond, D. G. Mechanistic Rationalization of Unusual Kinetics in Pd-Catalyzed C−H Olefination. *J. Am. Chem. Soc.* **2012**, *134*, 4600−4606.

(59) For reported examples of Pd-catalyzed ε-C−H functionalization, see: (a) Pearson, R.; Zhang, S.; He, G.; Edwards, N.; Chen, G. Synthesis of phenanthridines via palladium-catalyzed picolinamide-directed sequential C−H functionalization. *Beilstein J. Org. Chem.* **2013**, *9*, 891−899. (b) Wang, C.; Chen, C.; Zhang, J.; Han, J.; Wang, Q.; Guo, K.; Liu, P.; Guan, M.; Yao, Y.; Zhao, Y. Easily Accessible Auxiliary for Palladium-Catalyzed Intramolecular Amination of C(sp^2)−H and C(sp^3)−H Bonds at δ- and ε-Positions. *Angew. Chem., Int. Ed.* **2014**, *53*, 9884−9888. (c) Naveen; Rajkumar, V.; Babu, S. A.; Gopalakrishnan, B. Pd(II)-Catalyzed Bidentate Directing Group-Aided Chemoselective Acetoxylation of Remote ε-C(sp^2)−H Bonds in Heteroaryl−Aryl-Based Biaryl Systems. *J. Org. Chem.* **2016**, *81*, 12197−12211. (d) St John-Campbell, S.; Ou, A. K.; Bull, J. A. Palladium-Catalyzed C(sp^3)−H Arylation of Primary Amines Using a Catalytic Alkyl Acetal to Form a Transient Directing Group. *Chem.—Eur. J.* **2018**, *24*, 17838−17843.

(60) Using a mixture of **2** and **3b**, monitoring % D incorporation over time showed preferential deuteration at *cis*- and *trans*-C(4)−H bonds of **2**. In contrast, markedly reduced deuteration was observed for derivative **3b** at all reactive positions. See the Supporting Information for further details.

(61) Martínez-Carrión, A.; Howlett, M. G.; Alamillo-Ferrer, C.; Clayton, A. D.; Bourne, R. A.; Codina, A.; Vidal-Ferran, A.; Adams, R. W.; Burés, J. Kinetic Treatments for Catalyst Activation and Deactivation Processes based on Variable Time Normalization Analysis. *Angew. Chem., Int. Ed.* **2019**, *58*, 10189−10193.

(62) Hartman, M.; Svoboda, K.; Čech, B.; Pohořelý, M.; Šyc, M. Decomposition of Potassium Hydrogen Carbonate: Thermochemistry, Kinetics, and Textural Changes in Solids. *Ind. Eng. Chem. Res.* **2019**, *58*, 2868−2881.

(63) Prior optimization studies showed a detrimental effect of moisture, with optimal results obtained using flame-dried K_2CO_3. See ref 35.

(64) (a) Wang, X.-C.; Hu, Y.; Bonacorsi, S.; Hong, Y.; Burrell, R.; Yu, J.-Q. Pd(II)-Catalyzed C−H Iodination Using Molecular I_2 as the Sole Oxidant. *J. Am. Chem. Soc.* **2013**, *135*, 10326−10329. (b) Arroniz, C.; Denis, J. G.; Ironmonger, A.; Rassias, G.; Larrosa, I. An organic cation as a silver(I) analogue for the arylation of sp^2 and sp^3 C−H bonds with iodoarenes. *Chem. Sci.* **2014**, *5*, 3509−3514. (c) Campeau, L. C.; Parisien, M.; Jean, A.; Fagnou, K. Catalytic Direct Arylation with Aryl Chlorides, Bromides, and Iodides: Intramolecular Studies Leading to New Intermolecular Reactions. *J. Am. Chem. Soc.* **2006**, *128*, 581−590. (d) Ag salts have often been used as halide scavengers, see: Daugulis, O.; Zaitsev, V. G. Anilide *ortho*-Arylation by Using C-H Activation Methodology. *Angew. Chem., Int. Ed.* **2005**, *44*, 4046−4048. (e) Shabashov, D.; Daugulis, O. Catalytic Coupling of C−H and C−I Bonds Using Pyridine As a Directing Group. *Org. Lett.* **2005**, *7*, 3657−3659. (f) Chiong, H. A.; Pham, Q.-N.; Daugulis, O. Two Methods for Direct ortho-Arylation of Benzoic Acids. *J. Am. Chem. Soc.* **2007**, *129*, 9879−9884. (g) Lebrasseur, N.; Larrosa, I.

https://doi.org/10.1021/acscatal.3c01980
ACS Catal. 2023, 13, 9597−9615

Room Temperature and Phosphine Free Palladium Catalyzed Direct C-2 Arylation of Indoles. *J. Am. Chem. Soc.* **2008**, *130*, 2926−2927. (h) See ref 9a.

(65) Wisniewski, S. R.; Savage, S. A.; Romero, E. O.; Eastgate, M. D.; Tan, Y.; Simmons, E. M.; Plata, R. E.; Sowa, J. R.; Blackmond, D. G. Utilizing Native Directing Groups: Mechanistic Understanding of a Direct Arylation Leads to Formation of Tetracyclic Heterocycles via Tandem Intermolecular, Intramolecular C−H Activation. *J. Org. Chem.* **2019**, *84*, 7961−7970.

(66) He, J.; Li, S.; Deng, Y.; Fu, H.; Laforteza, B. N.; Spangler, J. E.; Homs, A.; Yu, J.-Q. Ligand-Controlled C(sp^3)−H Arylation and Olefination in Synthesis of Unnatural Chiral α−Amino Acids. *Science* **2014**, *343*, 1216−1220.

(67) Shao, Q.; Wu, K.; Zhuang, Z.; Qian, S.; Yu, J.-Q. From $Pd(OAc)_2$ to Chiral Catalysts: The Discovery and Development of Bifunctional Mono-N-Protected Amino Acid Ligands for Diverse C−H Functionalization Reactions. *Acc. Chem. Res.* **2020**, *53*, 833−851.

(68) Hill, D. E.; Yu, J.-Q.; Blackmond, D. G. Insights into the Role of Transient Chiral Mediators and Pyridone Ligands in Asymmetric Pd-Catalyzed C−H Functionalization. *J. Org. Chem.* **2020**, *85*, 13674−13679.

(69) For use of diaryliodonium salts (a) Kalyani, D.; Deprez, N. R.; Desai, L. V.; Sanford, M. S. Oxidative C−H Activation/C−C Bond Forming Reactions: Synthetic Scope and Mechanistic Insights. *J. Am. Chem. Soc.* **2005**, *127*, 7330−7331. (b) Deprez, N. R.; Sanford, M. S. Synthetic and Mechanistic Studies of Pd-Catalyzed C−H Arylation with Diaryliodonium Salts: Evidence for a Bimetallic High Oxidation State Pd Intermediate. *J. Am. Chem. Soc.* **2009**, *131*, 11234−11241. (c) See also ref 64d. (d) For use of diazonium salts: Biajoli, A. F. P.; da Penha, E. T.; Correia, C. R. D. Palladium catalysed regioselective arylation of indoles, benzofuran and benzothiophene with aryldiazonium salts. *RSC Adv.* **2012**, *2*, 11930−11935. (e) Gemoets, H. P. L.; Kalvet, I.; Nyuchev, A. V.; Erdmann, N.; Hessel, V.; Schoenebeck, F.; Noël, T. Mild and selective base-free C−H arylation of heteroarenes: experiment and computation. *Chem. Sci.* **2017**, *8*, 1046−1055. (f) Reay, A. J.; Hammarback, L. A.; Bray, J. T. W.; Sheridan, T.; Turnbull, D.; Whitwood, A. C.; Fairlamb, I. J. S. Mild and Regioselective $Pd(OAc)_2$-Catalyzed C−H Arylation of Tryptophans by $[ArN_2]X$, Promoted by Tosic Acid. *ACS Catal.* **2017**, *7*, 5174−5179.

(70) For a study on different monodentate pyridine-based DGs in the Pd-catalyzed C(sp^2)−H acetoxylation of aromatic rings, see: Desai, L. V.; Stowers, K. J.; Sanford, M. S. Insights into Directing Group Ability in Palladium-Catalyzed C−H Bond Functionalization. *J. Am. Chem. Soc.* **2008**, *130*, 13285−13293.

(71) The electronic requirements of the different coordinating sites of bidentate amide directing groups have been little studied, primarily with regard to the C−H activation step. For computational studies: (a) Tang, H.; Zhou, B.; Huang, X.-R.; Wang, C.; Yao, J.; Chen, H. Origins of Selective C(sp^2)−H Activation Using Transition Metal Complexes with N,N-Bidentate Directing Groups: A Combined Theoretical−Experimental Study. *ACS Catal.* **2014**, *4*, 649−656. (b) Tang, H.; Huang, X.-R.; Yao, J.; Chen, H. Understanding the Effects of Bidentate Directing Groups: A Unified Rationale for sp^2 and sp^3 C−H Bond Activations. *J. Org. Chem.* **2015**, *80*, 4672−4682. (c) For variations in the proximal binding site of (monodentate) auxiliary proposed to have an effect on the C−H activation step: Le, K. K. A.; Nguyen, H.; Daugulis, O. 1-Aminopyridinium Ylides as Monodentate Directing Groups for sp^3 C−H Bond Functionalization. *J. Am. Chem. Soc.* **2019**, *141*, 14728−14735.

(72) Examining the changes in partial charges on the coordinating nitrogen atoms of the directing group during the oxidative addition and reductive elimination steps by DFT indicated a relative positive charge buildup on the quinoline N atom during reductive elimination.

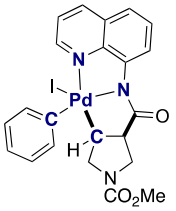

Change in charge density	Ox Add $I\text{-}2a_{cis}$ to $TS\text{-}OA_{cis}$	Red Elim $I\text{-}3_{cis}$ to $TS\text{-}RE_{cis}$
Pd	+0.05	−0.03
C(Ar)	+0.12	−0.08
C(alkyl)	+0.07	~0
N(amide)	−0.01	−0.02
N(pyr)	~0	+0.03

The changes in charges at the C(Ar) and C(alkyl) centers presumably relate to the influence of the change in the Pd oxidation state in the relative processes. Both steps see a small increase in electron density on the amide N. The oxidative addition step does not have a significant change in charge density for the quinoline N. In contrast, a notable increase in positive charge is observed at this position during reductive elimination, despite the increase in electron density on the Pd center. See the Supporting Information for further details. Charge stabilization by electron-donating groups at C4 on the quinoline directing group may be a factor in the improved yields with these examples (Scheme 6).

(73) It is noteworthy that this is a different effect to that observed by Daugulis, where a more electron-rich monodentate directing group was employed to promote reaction at secondary centers (ref 71c). As a mono-dentate directing group, this would affect the electronics of the proximal binding site and be proposed to have an effect on the C−H activation step.

(74) Mason, R. M. Studies on the Effect of Probenecid ("Benemid") in Gout. *Ann. Rheum. Dis.* **1954**, *13*, 120−130.

(75) Lee, Y. H.; Morandi, B. Metathesis-active ligands enable a catalytic functional group metathesis between aroyl chlorides and aryl iodides. *Nat. Chem.* **2018**, *10*, 1016−1022.

(76) Irby, C. E.; Yentzer, B. A.; Feldman, S. R. J. A Review of Adapalene in the Treatment of Acne Vulgaris. *Adolesc. Health* **2008**, *43*, 421−424.

(77) Welch, E. M.; Barton, E. R.; Zhuo, J.; Tomizawa, Y.; Friesen, W. J.; Trifillis, P.; Paushkin, S.; Patel, M.; Trotta, C. R.; Hwang, S.; et al. PTC124 targets genetic disorders caused by nonsense mutations. *Nature* **2007**, *447*, 87−91.

https://doi.org/10.1021/acscatal.3c01980
ACS Catal. 2023, 13, 9597−9615